

Abstract

Pål Westermark (2005). Models of the metabolism of the pancreatic beta-cell. Doctoral Thesis, School of Computer Science and Communication, Royal Institute of Technology, Stockholm, Sweden. Language: English. ISBN 91-7178-140-0

Keywords: pancreatic beta-cell, glucose stimulated insulin secretion, systems biology, metabolic modeling, metabolic control analysis.

The pancreatic β -cell secretes insulin in response to a raised blood glucose level. Deficiencies in this control system are an important part of the etiology of diabetes. The biochemical basis of glucose-stimulated insulin secretion is incompletely understood, and a more complete understanding is an important component in the quest for better therapies against diabetes.

In this thesis, mathematical modeling has been employed in order to increase our understanding of the biochemical principles that underlie glucose-stimulated insulin secretion of the pancreatic β -cell. The modeling efforts include the glycolysis in the β -cell with particular emphasis on glycolytic oscillations. The latter have earlier been hypothesized to be the cause of normal pulsatile insulin secretion. This model puts this hypothesis into quantitative form and predicts that the enzymes glucokinase and aldolase play important roles in setting the glucose concentration threshold governing oscillations. Also presented is a model of the mitochondrial metabolism in the β -cell, and of the mitochondrial shuttles that connect the mitochondrial metabolism to the glycolysis. This model gives sound explanations to what was earlier thought to be paradoxical behavior of the mitochondrial shuttles during certain conditions. Moreover, it predicts a strong signal from glucose towards cytosolic NADPH formation, a putative stimulant of insulin secretion. The model also identifies problems with earlier interpretations of experimental results regarding the β -cell mitochondrial metabolism. As an aside, an earlier proposed conceptual model of the generation of oscillations in the TCA cycle is critically analyzed.

Further, metabolic control analysis has been employed in order to obtain mathematical expressions that describe the control by pyruvate dehydrogenase and fatty acid oxidation over different aspects of the mitochondrial metabolism and the mitochondrial shuttles. The theories developed explain recently observed behavior of these systems and provide readily testable predictions.

The methodological aspects of the work presented in the thesis include the development of a new generic enzyme rate equation, the generalized reversible Hill equation, as well as a reversible version of the classical general modifier mechanism of enzyme action.

List of Papers

The present thesis builds on five original papers, referred to in the text by roman numerals I – V.

- Paper I.** Pål O. Westermark and Anders Lansner (2003). A model of phosphofructokinase and glycolytic oscillations in the pancreatic β -cell. *Biophysical Journal*, 85:126–139.
- Paper II.** Pål O. Westermark, Jeanette Hellgren Kotaleski, and Anders Lansner (2004). Derivation of a reversible Hill equation with modifiers affecting catalytic properties. *WSEAS Transactions on Biology and Medicine*, 1:91–98.
- Paper III.** Pål O. Westermark, Jeanette Hellgren Kotaleski, and Anders Lansner (2004). Glucose-stimulated insulin secretion — insights from modelling. *Recent Research Developments in Biophysics*, 3:325–350.
- Paper IV.** Pål O. Westermark, Jeanette Hellgren Kotaleski, Anneli Björklund, Valdemar Grill, and Anders Lansner (2005). A mathematical model of the mitochondrial NADH shuttles and anaplerosis in the pancreatic β -cell. *Submitted*.
- Paper V.** Pål O. Westermark (2005). On the metabolic control of pyruvate dehydrogenase and pyruvate carboxylase in the pancreatic β -cell. *Submitted*.

Abbreviations

The following frequently used abbreviations are also given in the text. Very commonly known biochemical compounds, e.g. ATP, NAD(H), etc. are given without explanation.

PDH	Pyruvate Dehydrogenase
NIDDM	Non-Insulin Dependent Diabetes Mellitus
ODE	Ordinary Differential Equation
MCA	Metabolic Control Analysis
GRH	Generalized Reversible Hill (equation)
TCA	Tricarboxylic Acid (cycle)
GSIS	Glucose-Stimulated Insulin Secretion
GO	Glucose Oxidation
FO	Fatty acid Oxidation
GK	Glucokinase
PFK	Phosphofructokinase
F6P	Fructose-6-Phosphate
FBP	Fructose-1,6-Bisphosphate
GPDH	Glyceraldehyde-3-Phosphate Dehydrogenase
PC	Pyruvate Carboxylase
CS	Citrate Synthase
MDH	Malate Dehydrogenase
IDH	Isocitrate Dehydrogenase, NAD-reducing
IDHP	Isocitrate Dehydrogenase, NADP-reducing
AAT	Amino Aspartate Transaminase
ACS	ATP-Citrate Synthase
MA	Malate-Aspartate (shuttle)
G3DH	Glyceraldehyde-3-phosphate Dehydrogenase
ME	Malic Enzyme
GDH	Glutamate Dehydrogenase
LC-CoA	Long-Chain Acyl-CoA
m (as in MDHm)	mitochondrial (as in mitochondrial MDH)
c	cytosolic

Acknowledgements

I thank my boss during the years at KTH, Anders Lansner, for conceiving the project, hiring me and letting me develop freely while always supporting me with exceptional scientific judgement. I thank Jeanette Hellgren for coming up with some excellent ideas at the right time and for being my roommate. I thank Örjan Ekeberg for all his generous and careful help and time concerning different topics, primarily computer related. I thank Erik Fransén for interesting discussions and help. I thank Anneli Björklund and Valdemar Grill for a great collaboration and for believing in the project. I thank Fredrik Edin for genuine and careful interest. I thank Anna Svantesson and Pål Nyrén for a great collaboration on a side project and Mikael Huss for some smaller collaborations that may turn out to yield something. I thank Martin Rehn for being a good course mate on a couple of graduate courses. I thank all other present and past people at (nowadays former) SANS for their contributions and for without exception being good colleagues. Here's hoping that I'll remain in professional and personal contact with you all in the future. Skål!

Thanks also to the PSCI institute at KTH for financial support, to the great administrator Harriett Johansson, to the manager Harald Hermansson and to Stephen James and Martin Norin at Biovitrum for interest and belief in the project.

Thanks to the thousands of developers behind the free software that I have used during the project: Debian GNU/Linux, GNOME, Mozilla, xppaut, Grace, Gnumeric, \LaTeX and \LyX come to my mind, among others.

These were only thanks of direct relevance for the thesis work. My family and friends are dearly loved, but you know that already, don't you. . .

A good deal of the material of this thesis was created listening to music; Bertrand Burgalat, Field Mice, Brian Eno, Harold Budd, Momus, Marvin Gaye, Serge Gainsbourg or Bernard Herrmann, for instance.

Contents

1	Introduction: Modeling the Biochemistry of the β-cell	1
1.1	Biochemical Background	3
1.2	Overview of the Thesis	7
2	Theory: Chemical Thermodynamics and Kinetics	8
2.1	Basic Chemical Thermodynamics	8
2.2	Enzyme Kinetics	9
	The Michaelis-Menten and Hill Equations	10
	The Generalized Reversible Hill Equation	13
3	Application: Modeling the Action of Single Enzymes	16
3.1	Phosphofructokinase	16
3.2	Malate Dehydrogenase	18
4	Theory: From the Parts to the Whole. Modeling, Analysis and Simulation of Biochemical Reaction Systems	22
4.1	Critical Assumptions	23
4.2	Metabolic Control Analysis (MCA)	24
4.3	The Method of Numerical Continuation	25
4.4	More Complex Behavior: from Steady State to Prolonged Oscillations	26
5	Application: The Glycolysis, NADH Shuttles and TCA Cycle	27
5.1	The Glycolysis	27
5.2	NADH Shuttles and TCA Cycle	31
	Modular MCA of the NADH Shuttle System	37
	MCA of the Anaplerosis	40
	On Oscillations in the TCA Cycle	44
6	Conclusions: Summary of Results and Suggestions for Further Investigations	47
6.1	Proposals for Further Research	49

Chapter 1

Introduction: Modeling the Biochemistry of the β -cell

This thesis is written mainly from a biochemical viewpoint. By that I mean that the problems that were explored are biochemical. On the other hand, the methods of exploration are mathematical and computational. The biochemical subject is the metabolism of the pancreatic β -cell, or more specifically, the metabolic events behind the glucose-stimulated insulin secretion (GSIS) these cells are specialized for. I have had the privilege of formulating mathematical models of the two most well-known biochemical pathways: the glycolysis and the tricarboxylic acid (TCA) cycle, which are important parts of GSIS, since the β -cell senses the need for insulin secretion via an increase in its basic glucose metabolism. The entire biochemical background is presented briefly in section 1.1 and more in detail in **paper III**.

The general subject of this thesis, referred to as theoretical biology, biophysics, or computational systems biology, is often regarded as multidisciplinary. I believe that this is about to change. As quantitative methods from physics, chemistry, mathematics and computer science prove more and more practically useful in biology and medicine, these disciplines will assimilate quantitative methods to an extent that they will be regarded as indispensable parts of the subjects, not as interdisciplinary excursions from the mainstream. Every human being is occupied with building models of his or her surroundings, consciously or not. Also the empirical biochemist uses conceptual models and corresponding assumptions when interpreting and presenting the information he or she gathers. There is no naive or unfiltered eye. Certainly, any kind of scientific thinking involves making explicit, in one way or another, theoretical models, which serve to make us understand the reality, and to predict future events. In practical scientific work, theory is indispensable in interpreting empirical observations, and guiding the scientist when figuring out which experiments to conduct in the future. In a broader perspective, theory represents an integral part of the reductionist paradigm, in the sense that it defines the rules which explain how phenomena observed at one level of description relate to phenomena at another level. Usually, one may pose this as the rules for how the behaviour of the parts relates to the behavior of the whole, and vice versa.

The means with which theories are made explicit vary. Traditionally, biologists use plain language (English) to formulate biological theories. However, symbolic reasoning is not well suited for making sense of the way the behavior of the parts relates to the behavior of the whole. How entities like enzymes and metabolites relate to the dynamical behavior of a system consisting of sets of these entities is best analyzed with mathematical methods. Thus, in this thesis, mathematics is employed to formulate the core of the theoretical models. It is my conviction that formulating a biological model in quantitative mathematical terms gives it qualitatively superior predictive power. It also forces the biologist to make explicit many assumptions usually not needed to address when using plain language, simply because plain language lacks the precision needed to lure these assumptions out of their dwellings. This, especially in the biological and medical sciences, can be quite painful but healthy.

As an example, consider a simple model system consisting of an enzyme which is activated by its product (this kind of enzyme is unusual but probably plays an important role in GSIS, see **paper I**). Its substrate is produced with a constant rate, and its product is removed with a rate proportional to its concentration. The biochemist inclined to use verbal descriptions may imagine a scenario where the substrate and product concentrations attain a steady-state. He or she may also imagine a scenario where the concentrations vary cyclically. The product activation of the enzyme causes the product to accumulate and the substrate to deplete until the point where the substrate concentration is too low to uphold any significant product formation. The product concentration will now fall, the substrate concentration will rise, and product activation of the enzyme will again occur. Nothing in this verbal description tells us which conditions that will make each one of the scenarios occur. However, by formulating this description mathematically (see **paper I**) we learn that steady-states occur at both low and high substrate production rates, while an oscillatory state occurs at intermediate production rates.

The way to a useful mathematical model is however anything but easy or quick. I would like to address two, sometimes contradicting, virtues of a theoretical model:

- The model should be as simple as possible
- The model should relate to empirical data in a clear and unambiguous way

Both these virtues are problematic and difficult to assess. The first builds on a tradition in western art, science and poetry, well summarized by Horace in *Ars Poetica* (circa 18 BC):

Denique sit quod vis, simplex dumtaxat et unum

— “Let [the work] be what you will, at least let it be simple and one”. Especially in physics, Horace’s maxim is still an aesthetic guiding principle. One may even regard Occam’s razor as a rationalized formulation of this principle. Regardless of the aesthetic aspects, simplicity makes the important assumptions clear and helps reveal the underlying principles and logic of a model. A model does not necessarily gain sophistication if it adds details that do not contribute essentially to its logical structure or qualitative behavior. A more practical aspect in the field of biochemical modeling is simplicity in the sense that the

number of parameters often has to be kept as low as possible, since measured biochemical parameters usually are marred with significant uncertainties. An exploration of parameter space quickly becomes practically impossible as the number of parameters rises. This is the “curse of dimensionality”.

Here, however, it is pertinent to consider the second virtue. The quest for simplification may clash with the desire for a description that is in line with empirical observations. One may drive simplifications too far and discard vital empirical knowledge. It is an advantage if the parameters of the equations one uses are directly observable or at least derived unambiguously from observable entities. In this case it is, even though the parameters are uncertain, straightforward to estimate probable physiological *ranges* of them. From these, one may infer extreme cases or scenarios, and with the aid of methods from experimental design [1] find good strategies to tackle the curse of dimensionality.

This is a possible starting point for attempts to rationalize the level of detail of models. However, in the biological sciences, the optimal level of detail varies from question to question, from system to system, and to my mind it is at this stage of the scientific development mostly a matter of judgement or simply taste. During such circumstances, an open mind is a valuable asset.

1.1 Biochemical Background

The human body needs to maintain a steady blood glucose level. In response to raised blood glucose, the pancreatic β -cells secrete insulin into the bloodstream, which acts as a signal for tissues to take up and break down glucose. Failure of this control system to work properly may result in a state of chronic hyperglycemia commonly known as diabetes mellitus. The most common form of diabetes is type 2 or *non-insulin dependent diabetes mellitus* (NIDDM), which is estimated to affect 3–4% of the Swedish population [2], and in a global perspective more than 6% of the population of the developed world and about 3.5% of the population of developing countries [3]. The etiology of NIDDM is complex. Two main factors behind the disease emerge: first, *insulin resistance*, the impairment of tissue sensitivity to insulin, and second, *insulin deficiency*, an impaired capability of the β -cells to secrete insulin in response to glucose and other secretagogues. Both these factors may have both genotypic and phenotypic origins. The successive progression of a healthy subject towards a diabetic state may be divided into four steps [4]: 1) Normal glucose homeostasis. 2) Disturbed glucose homeostasis. There is insulin resistance, which is compensated by an increased secretory response by the β -cells, due to an increased total β -cell mass and possibly an increased insulin secretion per cell. 3) Impaired glucose homeostasis. The blood glucose level is increased, due to both insulin resistance and insulin deficiency, due to loss of β -cell mass and impaired glucose sensitivity of the remaining β -cells, which exhibit an attenuated first or acute insulin secretion phase. 4) The chronic diabetic state, with a roughly 50% reduced β -cell mass and an even more impaired secretory capacity of the remaining β -cells. The pulsatility of the insulin secretion (see below) is here distorted. Common to stages 3 and 4 is the dedifferentiation of the β -cells, i.e. the loss of important peculiarities in the gene expression profile. In conclusion, the importance of insulin deficiency in the etiology of NIDDM makes the understanding of the biochemistry of GSIS a high priority.

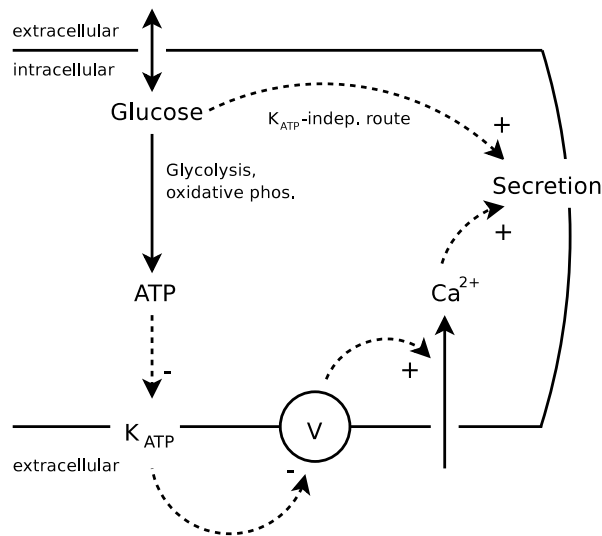


Figure 1.1: **The K_{ATP} -dependent pathway** comprises glucose increasing the ATP/ADP ratio which closes ATP-sensitive K^+ channels. This results in a depolarization of the cell membrane (V indicates membrane potential). In response to this, voltage-sensitive Ca^{2+} channels open, which leads to an increased $[Ca^{2+}]_i$, which in turn stimulates insulin secretion. A K_{ATP} -independent pathway acts synergistically.

The β -cells are localized in small clusters of about 2000–3000 cells: the islets of Langerhans. These clusters are scattered throughout the pancreas and amount to about a million, comprising a few percent of the total pancreatic mass [5]. The cells in an islet are coupled electrically and chemically via gap-junctions to form a syncytium. The β -cells quickly equilibrate their intracellular glucose concentration with that of the surrounding blood, and are able to gauge their insulin secretion rate accordingly. The intracellular events leading from a raised intracellular glucose level to insulin secretion are interconnected in an intricate biochemical network. Much is now known about the parts of this network, less is known about how the parts determine its functioning as a whole. The ambition behind all the works in this thesis has been to gain a better understanding of the relation between the parts and the whole of the biochemistry of GSIS.

Our basic understanding of β -cell GSIS is depicted in figure 1.1. The β -cell “senses” the glucose level via its metabolic rate. The key is that an increased glucose concentration will increase the glycolytic flux. This will increase the cytosolic ATP/ADP ratio, which closes ATP sensitive K channels (K_{ATP} -channels). This causes the cell membrane to depolarize, which leads to Ca^{2+} influx into the cytosol via voltage-sensitive Ca^{2+} -channels. Secretion of insulin via secretory vesicles is now stimulated by the increased Ca^{2+} concentration. This signalling pathway is usually referred to as the K_{ATP} -dependent pathway and is today thought to be necessary for insulin secretion [6].

Complex dynamical patterns The electrical activity of the β -cell exhibits complex temporal dynamics. The ATP-induced depolarization of the membrane potential is not tonic, instead it has the form of repetitive bursting. The bursts consist of depolarized plateaus of about -30 to -40 mV, on which spikes (action potentials) of about 10 – 20 mV are superimposed. Between these bursts are hyperpolarized phases of about -60 to -50 mV [7]. To complicate matters further, there are two different main characteristic burst frequencies: “Medium bursting”, with a period of 10 – 60 s and “slow bursting” with a period of 2 – 4 min. These are seen in both single cells and in whole islets, synchronized throughout the syncytium. Synchronized with this bursting activity are oscillations in intracellular Ca^{2+} concentration ($[\text{Ca}^{2+}]_i$). Crucially, insulin secretion is oscillatory as well, both *in vivo* [8] and *in vitro* [9], with a period of several minutes, and synchronized with slow bursting and corresponding $[\text{Ca}^{2+}]_i$ oscillations [10].

It is clear that the pulsatory insulin release pattern is of importance for the action of insulin on its target organs and tissues, especially the liver glucose metabolism [11]. Pulsatory release is the most common release mode for hormones [12] which has prompted some investigators to probe the reason for such release patterns. Receptor desensitization has been proposed as a molecular mechanism involved in an interplay with oscillatory hormone levels in the cases of gonadotropin-releasing hormone in humans and cAMP signaling in *Dictyostelium discoideum* [13], and it is plausible that a similar mechanism is at work in the case of hepatic insulin receptors [14]. However, the effects of insulin pulsatility on different aspects of hepatic metabolism are still to be elucidated fully. A recent study indicates that insulin pulsatility has little effect on liver glucose uptake [15], which would lead to the tentative conclusion that the effect rather is on liver glucose production.

A hypothesis that has been advocated the last decade [16] is that oscillations in the glycolysis underlie these minute-scale oscillations. A mathematical model of the β -cell glycolysis was created and analyzed during the course of this project, this is reported below (section 5.1) and in **paper I**.

A second signalling pathway The K_{ATP} -dependent pathway has been known for more than 20 years (see **paper III** for a review). An interesting development took place during the last decade, when it was revealed that there is a second pathway of GSIS which does not involve the K_{ATP} channel: the K_{ATP} -independent pathway. This pathway acts synergistically with the K_{ATP} -dependent pathway, and exhibits a slower response to a glucose bolus. The overall result is a biphasic insulin response to glucose: a first secretion pulse beginning in seconds after a glucose bolus, followed by a second sustained phase of pulses of insulin secretion with a higher basal secretory rate, as both pathways are fully operative.

The nature of the K_{ATP} -independent pathway is widely debated. Thought to be crucial is the concept of *anaplerosis*, i.e. the net influx of carbons to the TCA cycle. Anaplerosis is believed to occur mainly via the carboxylation of pyruvate accomplished by the enzyme pyruvate carboxylase (PC). This reaction produces oxaloacetate. The anaplerosis must, to avoid the catastrophic accumulation of TCA cycle intermediates, be counterbalanced by *cataplerosis*, the net removal of TCA cycle carbons. Different cataplerotic products are thought

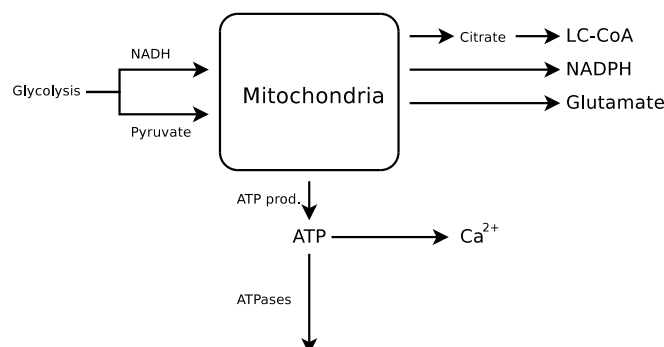


Figure 1.2: **The mitochondria relay the glycolytic signals** (pyruvate and NADH) to ATP (the K_{ATP} -dependent pathway) as well as to the K_{ATP} -independent pathway. The latter pathway consists of a yet unresolved signal, perhaps LC-CoA, NADPH, glutamate, or a combination of these compounds. Several feedback loops exist in this system. ATP and citrate inhibit glycolysis. Ca^{2+} stimulates ATPases and has a disputed effect on mitochondrial metabolism and oxidative phosphorylation.

to act as signals in the K_{ATP} -independent pathway. Three main hypotheses involving anaplerosis emerge from the recent literature on the subject:

1. There is a cataplerotic export of the TCA cycle intermediate citrate from the mitochondria. The citrate is in the cytosol cleaved to oxaloacetate and ac-CoA by the enzyme ATP-citrate synthase (ACS). The ac-CoA is transformed to malonyl-CoA, which inhibits the mitochondrial long-chain acyl-CoA (LC-CoA) transporter. This increases cytosolic LC-CoA levels, which augments the Ca^{2+} stimulated insulin release via protein acylation [17, 6] as well as via DAG formation [18] which via protein kinase C activation promotes insulin secretion [19].
2. There is a cataplerotic export of the TCA cycle intermediate malate from the mitochondria. The malate is decarboxylated to pyruvate by the malic enzyme (ME) in the cytosol, under the reduction of cytosolic NADP to NADPH. NADPH is proposed to augment the Ca^{2+} stimulated insulin release either via direct action on the insulin secretory granules [20] or via further metabolism [21, 22] of NADPH.
3. There is a cataplerotic conversion of the TCA cycle intermediate 2-oxoglutarate to glutamate by the enzyme glutamate dehydrogenase (GDH). The glutamate is exported to the cytosol, where it is proposed to augment the Ca^{2+} stimulated insulin release via uptake by the insulin secretory granules [23, 24].

These three hypotheses are summarized in figure 1.2. The hypotheses are all controversial; counter-evidence to the first and third exist [25, 26] and no direct evidence has yet been found for the second hypothesis.

1.2 Overview of the Thesis

The general aim of the present thesis is to fill gaps in the theoretical understanding of the biochemistry of the β -cell. Specifically, the β -cell glycolysis has been modeled and the hypothesis of an oscillatory β -cell glycolysis has been given a quantitative form. Moreover, the mitochondrial metabolism has been modeled and analyzed both numerically and analytically. The signaling from an increased glycolytic flux to the three putative messengers of the K_{ATP} -independent pathway outlined above has been simulated. A general aim has been to propose biochemically meaningful predictions based on the models, predictions that are experimentally testable with today's technology. Finally, the toolbox of metabolic modeling has been extended with a new generic rate equation.

The structure of this thesis is as follows. In *chapter 2*, the theoretical foundation for the understanding of the kinetics of single enzymes is outlined. In addition to established theory, this chapter includes a summary of the results of **paper II**, where a new generic rate equation is derived.

In *chapter 3*, the general reversible Hill equation is applied to the enzyme phosphofructokinase. These results were published in **paper II**. Also, a specific rate equation for mitochondrial malate dehydrogenase is developed. The results can partially be found in **paper IV**, although this section contains a significant deal of original results not presented elsewhere.

Chapter 4 takes the step towards a view from a higher systemic level. The state of the art in the theory of modeling metabolic networks is introduced. Specific topics include metabolic control analysis (MCA), stability analysis and the numerical method called continuation. Also included is a section describing five seldom mentioned but often implicitly made assumptions that are, to this writer's mind, critical.

Chapter 5 is long and includes summaries of the model of β -cell glycolysis created in **paper I**, of the model of mitochondrial metabolism that is the subject of **paper IV**, and of the analytic treatment of the interface between the glycolysis and the mitochondrial metabolism presented in **paper V**. Main conclusions and predictions of these works are summarized. Furthermore, the chapter contains some original unpublished work that cannot be found in the five original papers of the thesis: a modular metabolic control analysis of the model presented in **paper IV**, as well as a theoretical evaluation of a recent hypothesis of the mechanism behind the generation of oscillations in the mitochondrial metabolism.

The thesis ends with *chapter 6* where a general summary is given, together with suggestions for future work.

Chapter 2

Theory: Chemical Thermodynamics and Kinetics

This chapter presents the natural laws from chemical thermodynamics and kinetics that constitute the foundation of the models in this thesis, and of a great deal of the entire scientific field of metabolic and electrophysiological modeling for that matter. The principles of thermodynamics set the constraints that determine the direction of chemical reactions, i.e. the sign of the net reaction rate, while kinetics determine the absolute value of the reaction rate. The core of the models of β -cell biochemistry presented in this thesis are quantitative descriptions of different enzymes. These are generic models (rate equations) describing the action of single enzymes, and these rate equations build on the basic principles of chemical thermodynamics and kinetics. In addition to the established theory, a new generic rate equation, the general reversible Hill equation, derived in **paper II**, is described.

2.1 Basic Chemical Thermodynamics

A rigid requirement for a quantitative model of a set of chemical reactions is that the basic laws of thermodynamics are followed. Let us consider a system composed of n chemical species. The law of mass action allows us to write the equilibrium constant K_{eq} for any chemical reaction:

$$K_{\text{eq}} = \prod_{i=1}^n S_i^{-\nu_i}, \quad (2.1)$$

where S_i usually is the equilibrium concentration of species i (in order for equation (2.1) to be exact, S_i should represent the *activity* of species i , which often is well approximated by the concentration), and where ν_i is the stoichiometric number of reactant i , positive for substrates and negative for products. The equilibrium constant is related to the standard Gibb's free energy change ΔG° of the reaction through the relation

$$\Delta G^\circ = -RT \ln K_{\text{eq}}, \quad (2.2)$$

where R is the gas constant, T is the temperature, and where ΔG° is related to the standard Gibb's free energies of formation $\Delta_f G_i^\circ$ of the species involved in the reaction:

$$\Delta G^\circ = \sum_i \nu_i \Delta_f G_i^\circ \quad (2.3)$$

In general, the reactions of living systems are far from equilibrium, i.e. equation 2.1 is *not* fulfilled. Still, in case of, for instance, biochemical reactions taking place within the cytosol of a living cell where concentration gradients are not too large and where reactive collisions between molecules are sufficiently rare, a local entropy may be defined [27], and the molar free energy change of a reaction may be written

$$\Delta G = \Delta G^\circ + RT \ln \Gamma = RT \ln \frac{\Gamma}{K_{\text{eq}}}, \quad (2.4)$$

where Γ is the mass action ratio (the quotient of the actual concentrations of the species), written in the same form as for K_{eq} above. Equation 2.4 determines in which direction a reaction will proceed (macroscopically) given the concentrations of substrates and products, that is, the second law of thermodynamics is valid in this local thermodynamic picture: the local entropy always increases if we are not in equilibrium. If $\Delta G < 0$, the reaction will favor consumption of substrates and production of products. If $\Delta G > 0$, the opposite holds.

Thus, biochemical reactions can be said to be under a potential, a fact which greatly facilitates the theoretical understanding of them. The signs of the rate equations that describe the rates of the chemical reactions in a cell must satisfy equation 2.4, which, as we will see, leads to equation 2.8. Hence, given the concentrations of the reactants of a reaction together with the equilibrium constant, we may be sure of the direction in which the net reaction takes place. Most importantly, the $\Delta_f G_i^\circ$ values of many common metabolites found inside a cell have been tabulated [28, 29, 30]. The modeling efforts in this thesis have made extensive use of these tables in order to obtain consistent sets of equilibrium constants.

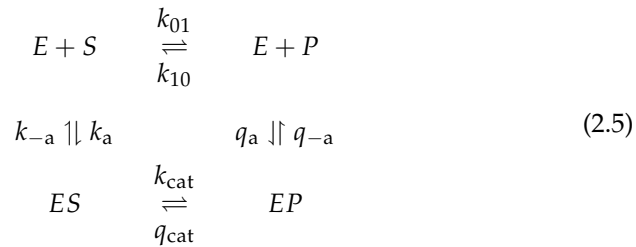
2.2 Enzyme Kinetics

While the laws of thermodynamics determine the *direction* of chemical reactions in a given environment, reaction *rates* are determined by the laws of chemical kinetics and are almost always determined in part by the concentrations of the reactants and possibly other compounds present. The core of the metabolic models in this thesis are rate equations which, using arguments from the theory of chemical kinetics, describe the flux-concentration relationships of enzyme catalyzed reactions while at the same time strictly adhering to the laws of thermodynamics. Here I give a survey of the methods and models of enzyme kinetics that have been put to use in the present thesis. I limit myself to describe generic rate equations that are applicable to a wide range of enzymes. These rate equations are in turn the reversible Michaelis-Menten

model, the reversible Hill equation and the generalized reversible Hill equation which was derived in **paper II**. A common trait of these equations is that their parameters are operationally well-defined — they reflect unambiguously the degrees of freedom often empirically found in the flux-concentration relationships. This comes at the expense of mechanistic detail: the equations build on simplified models of the enzymatic reactions. However, estimations of the values of parameters in more complicated rate equations are seldom available, and I find it imperative that quantitative descriptions in biophysical modeling are kept on a level where empirical data exist.

The Michaelis-Menten and Hill Equations

As a starting point, consider the following scheme of an enzyme catalyzed reaction:



where E denotes enzyme, S denotes substrate, P denotes product and ES and EP denotes enzyme-substrate and enzyme-product complex, respectively, and where the k s and q s are conventional rate constants.

The Reversible Michaelis-Menten Model We now follow Briggs and Haldane [31] and make the quasi-steady-state assumption that the condition

$$\frac{dES}{dt} = \frac{dEP}{dt} = 0$$

is attained on a much faster time-scale than that of the overall reaction. In this picture, we consider two steady-state fluxes, one from S to P , j_f , and one from P to S , j_r . One finds that the net reaction flux $j = j_f - j_r$ can be expressed as

$$j = \frac{E_0}{1 + S/K_{mS} + P/K_{mP}} \left(S \frac{k_{\text{cat}}}{K_{mS}} - P \frac{q_{\text{cat}}}{K_{mP}} \right), \tag{2.6}$$

where $K_{mS} = (k_{\text{cat}} + k_{-a})/k_a$ and $K_{mP} = (q_{\text{cat}} + q_{-a})/q_a$ are the Michaelis constants for the forward and reverse reactions, respectively, and where $E_0 = E + ES + EP$ is the total concentration of the enzyme. Introducing the parameters $V_f = E_0 k_{\text{cat}}$, $V_r = E_0 q_{\text{cat}}$, $\sigma = S/K_{mS}$ and $\pi = P/K_{mP}$ we can write the equation more compactly as

$$j = \frac{V_f \sigma - V_r \pi}{1 + \sigma + \pi}. \tag{2.7}$$

We can elegantly relate equation (2.7) to the equilibrium constant K_{eq} of the reaction (which depends solely of the $\Delta_f G^\circ$ values of the substrates and products) by noticing that $j = 0$ at equilibrium, which means that $V_f \sigma = V_r \pi$ which in turn can be rearranged to the important Haldane relationship:

$$\frac{V_f K_{mP}}{V_r K_{mS}} = K_{eq}. \quad (2.8)$$

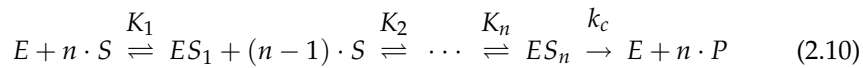
Using the Haldane relationship we write (2.7) in normalized form:

$$\frac{j}{V_f} = \frac{\left(1 - \frac{\Gamma}{K_{eq}}\right) \sigma}{1 + \sigma + \pi}. \quad (2.9)$$

This equation explicitly states that the reaction rate drops to zero at equilibrium, when $\Gamma/K_{eq} = 1$. In the irreversible case (i.e. in the limit when $\pi \rightarrow \infty$), $j/V_f = 1/2$ when $S = K_{mS}$. This point is referred to as the half-saturation point which may be used as an operational definition of K_{mS} .

The Michaelis-Menten equation is quite general, and applies to any reaction that is first order in the enzyme-substrate (and/or enzyme-product) complex; k_{cat} may in reality be a constant representing several steps of catalysis lumped together. Further, the mathematical form of the Michaelis-Menten equation is indistinguishable from the equation obtained if assuming that $E + S$ and ES , as well as EP and $E + P$, attain equilibrium instantaneously, which was the assumption originally made by Michaelis and Menten [32]. The Michaelis constants are then interpreted as dissociation constants. Indeed, this assumption of *quasi-equilibrium* is quite fruitful and was formalized by Cha [33], and it is the assumption made in most of the following derivations of rate equations.

The Hill Equation We may generalize equation 2.9 to a situation where the enzyme can bind the substrate at n sites, each binding of a substrate molecule facilitating the binding of the next one, a behaviour called positive cooperativity. This would yield the following scheme



where we require that the equilibrium constants satisfy $K_1 < K_2 < \cdots < K_n$ in order to have positive cooperativity throughout the reaction. In the extreme, all intermediary steps can be ignored which yields the important Hill equation of enzyme action

$$\frac{j}{V} = \frac{\sigma^n}{1 + \sigma^n} \quad (2.11)$$

When $n \neq 1$, the term Michaelis constant is not used, and we instead only use the term half-saturation point $S_{0.5}$. Note that the parameters V and $S_{0.5}$ have the same operational meaning as in the Michaelis-Menten model, but although the physical interpretation in terms of equilibrium constants made above (scheme 2.10) is possible it is not necessarily true: the Hill equation is usually regarded as a purely empirical equation, and we may let n assume non-integer values, in which case we use the Hill coefficient h in place of n . The relationship between substrate concentration and flux for the Hill equation is shown in figure 2.1.

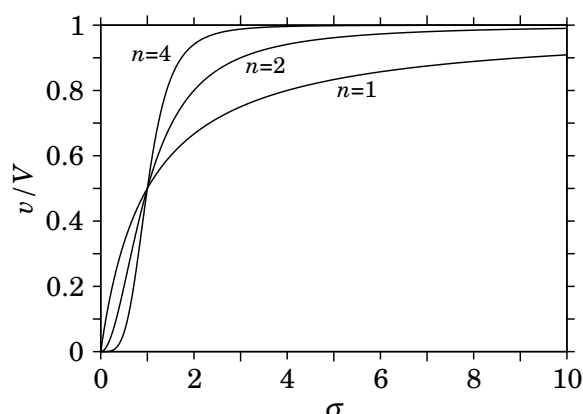


Figure 2.1: The relationship between substrate concentration and reaction flux exhibited by the Hill equation for different values of the parameter n . Note that $j = V/2$ when $S = S_{0.5}$ for all values of n and that the sigmoid curve is steeper with increasing n . We may use h , which may have non-integer values, instead of n .

We see that the flux-concentration curve is sigmoid-shaped, a sigmoid which becomes steeper with increasing n . The curve approaches a step function as n approaches infinity. It is also important to note that the Hill equation reduces to the irreversible Michaelis-Menten equation if $n = 1$, which thus operationally can be regarded as a special case of the more general Hill equation.

The Reversible Hill Equation In 1997, a reversible generalization of the irreversible Hill equation was derived [34]. This rate equation addresses the modulation of enzyme activity by modifiers, which can be any chemical species capable of binding to the enzyme and by doing so alters the enzyme's properties with respect to its substrates and products: modifiers may be inhibitors or activators. There are many different molecular mechanisms that can produce activation or inhibition. The reversible Hill equation only accounts for modifiers that affect the binding properties of the substrates and products to the enzyme. Denoting the modulator X , the dissociation constant for the binding of X to the enzyme $X_{0.5}$ and denoting the normalized modulator concentration $\xi = X/X_{0.5}$, the reversible Hill equation is written

$$j = \frac{V_f \sigma \left(1 - \frac{\Gamma}{K_{\text{eq}}}\right) (\sigma + \pi)^{h-1}}{(\sigma + \pi)^h + \frac{1 + \xi^h}{1 + \alpha \xi^h}}, \quad (2.12)$$

where α is inversely related to the factor a by which the modulator changes the affinity of the substrate for the enzyme: $\alpha = a^{-2h}$. The operational meaning of the parameter α was elucidated in **paper I** and **II**: $\lim_{\xi \rightarrow \infty} \frac{1 + \xi^h}{1 + \alpha \xi^h} = 1/\alpha$. In the irreversible case (i.e. $K_{\text{eq}} \rightarrow \infty$ and $\pi \rightarrow 0$), the modifier simply alters the effective half-saturation point with a factor $\alpha^{-1/h}$. This makes it easy to identify the factor α directly from empirically found flux-concentration curves. In the important case that $\alpha = 0$, we have competitive inhibition, which is the

case if the inhibitor only binds to enzyme molecules that have not bound any substrate molecules. This is the case if the substrate and modulator compete for the same binding site on the enzyme.

The Generalized Reversible Hill Equation

The reversible Hill equation derived by Hofmeyr and Cornish-Bowden [34] only accounts for reactions with one substrate and one product. Also, the reversible Hill equation lacks the ability to account for modifiers affecting the catalytic properties (i.e. modifiers altering the limiting rate V) — the modulators are assumed only to alter the affinities of substrates and products for the enzyme. In **paper II**, a generalization of the reversible Hill equation, namely the generalized reversible Hill (GRH) equation, was derived. This was done in order to alleviate the limitations of the reversible Hill equation. The motivation for this was the desire for a general equation able to describe the flux-rate relationships for the broad class of enzymes for which the catalytic mechanism is unknown or ambiguous, or for which the known mechanism leads to too complicated rate equations with parameters that have not been measured. The GRH equation describes modulator effects using parameters that are operationally well defined in the sense that they usually are easy to infer from experimental data. Another way to state this is that the parameters in an unambiguous way reflect the degrees of freedom usually observed. To the list of parameters of the reversible Hill equation: V , K_{eq} , $S_{0.5}$, $P_{0.5}$, $X_{0.5}$, α and h , we add one more: γ , which represents the factor by which the modulator changes the apparent limiting rate of the reaction.

We start by considering enzyme E consisting of two subunits, each capable of binding a substrate molecule S or product molecule P , as well as binding an allosteric modifier X . This is exactly the same situation as that considered by Hofmeyr and Cornish-Bowden [34], with the exception that we here allow the allosteric modifier to alter the catalytic properties of the enzyme as well as the binding of the substrate and product molecules. We thus arrive at the generic scheme in figure 2.2.

We assume quasi-equilibrium of the different reactions in figure 2.2, apply the venerable method of Cha [33], which is still going strong [35], and obtain for the rate of product formation j (see **paper II** for methods of derivation):

$$j = \frac{\frac{1+\gamma\alpha\xi^2}{1+\alpha\xi^2} V_f \sigma \left(1 - \frac{\Gamma}{K_{\text{eq}}}\right) (\sigma + \pi)}{(\sigma + \pi)^2 + \frac{1+\xi^2}{1+\alpha\xi^2}}$$

For an arbitrary Hill coefficient h ,

$$j = \frac{\frac{1+\gamma\alpha\xi^h}{1+\alpha\xi^h} V_f \sigma \left(1 - \frac{\Gamma}{K_{\text{eq}}}\right) (\sigma + \pi)^{h-1}}{(\sigma + \pi)^h + \frac{1+\xi^h}{1+\alpha\xi^h}}. \quad (2.13)$$

One may note that $\lim_{\xi \rightarrow \infty} \frac{1+\gamma\alpha\xi^h}{1+\alpha\xi^h} = \gamma$. Thus, the modifier simply alters the effective limiting rate with a factor γ . Just as in the case of the parameter α , the parameter γ is easy to infer from experimental flux-concentration curves. The estimation of the parameter $X_{0.5}$ is unfortunately more difficult to obtain.

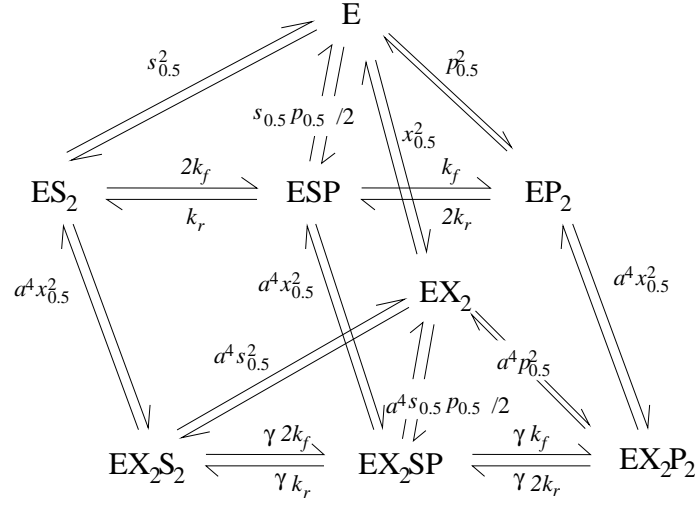


Figure 2.2: **The reaction scheme considered in the generalized reversible Hill equation.** The different equilibrium constants are indicated, as well as the catalytic constants (k_f and k_r). The factor a represents altering of the equilibrium constants by the modifier X , while the factor γ represents altering of the catalytic constants by the modifier. The intermediate binding steps (e.g. the ES complex) are neglected in order to obtain simple equations.

Unless $h = 1$, it is generally not possible to find plots from which it is possible to estimate this parameter directly. Some strategies for the estimation of this parameter are discussed in **paper I** and **II**. I also remark that if we let $V_r \rightarrow 0$ and $p_{0.5} \rightarrow \infty$, and set $\gamma = 0$ and $h = 1$, we obtain

$$j = \frac{V_f \sigma}{\sigma(1 + \alpha\xi) + 1 + \xi},$$

which is the well-known rate equation for linear mixed inhibition [36, 37].

Generalizing equation 2.13 to account for an arbitrary number of modifiers, some of which may share the same site, leads to¹:

$$j = \frac{\left(\prod_i \frac{1 + \sum_j \gamma_{ij} \alpha_{ij} \xi_{ij}^h}{1 + \sum_j \alpha_{ij} \xi_{ij}^h} \right) V_f \sigma \left(1 - \frac{\Gamma}{K_{eq}} \right) (\sigma + \pi)^{h-1}}{(\sigma + \pi)^h + \prod_i \frac{1 + \sum_j \xi_{ij}^h}{1 + \sum_j \alpha_{ij} \xi_{ij}^h}}, \quad (2.14)$$

where modifier site i may be acted upon by several modifiers X_{ij} . It should be noted that it is assumed that modifiers that bind to different sites do so independently.

We may generalize equation 2.12 further to let it describe reactions with several substrates and products, if no modifiers are considered. We assume that a substrate-product pair S_1 and P_1 may bind to their corresponding sites

¹The reader may note that regrettably, the summation signs were erroneously placed in paper II.

independently of another substrate-product pair S_2 and P_2 and vice versa. The forward reaction is assumed to take place only when all substrates have bound to their sites, and vice versa for the backward reaction and products. Accounting for an arbitrary number of substrate and product pairs, we write

$$j = \frac{V_f \prod_i \sigma_i \left(1 - \frac{\Gamma}{K_{eq}}\right) \left(\prod_i \sigma_i + \prod_j \pi_j\right)^{h-1}}{\prod_i \left(1 + (\sigma_i + \pi_i)^h\right)}.$$

Unfortunately, there is no compact expression if we include modifier effects since the denominator becomes impossible to factorize. In the special case when each modifier affects the binding and catalysis of one substrate and product pair *only*, we may write

$$j = \frac{\prod_k \left(\prod_i \frac{1 + \sum_j \gamma_{kij} \alpha_{kij} \xi_{kij}^h}{1 + \sum_j \alpha_{kij} \xi_{kij}^h} \right) V_f \prod_k \sigma_k \left(1 - \frac{\Gamma}{K_{eq}}\right) \left(\prod_k \sigma_k + \prod_l \pi_l\right)^{h-1}}{\prod_k \left(\prod_i \frac{1 + \sum_j \xi_{kij}^h}{1 + \sum_j \alpha_{kij} \xi_{kij}^h} + (\sigma_k + \pi_k)^h \right)}. \quad (2.15)$$

To summarize, the rate equations outlined in this chapter represent idealized cases. Their main advantage is that the degrees of freedom in their parameter spaces are well mapped to the degrees of freedom that are usually directly observable in experimental data. Uncertainties and natural variability in the empirical data are then possible to incorporate into the modeling enterprise in a straightforward manner. Because of this, I believe that the equations are suitable starting points for modeling work on multienzyme systems representing an *in vivo* situation, where kinetic detail of the single enzyme is of less interest than the collective behavior at the systemic level.

Chapter 3

Application: Modeling the Action of Single Enzymes

The theory outlined in chapter 2 is here given concrete form: the catalytic actions of two enzymes, phosphofructokinase (PFK) and malate dehydrogenase (MDH) are given quantitative descriptions. PFK is part of the glycolysis, and it turned out to be particularly challenging to find a rate equation for this enzyme. MDH is part of the TCA cycle, and of the enzymes in this pathway, MDH was the most difficult one to describe quantitatively. The single enzyme models described here were developed in **paper II** (PFK) and **paper IV** (MDH). The latter model is described in greater detail here below and is somewhat elaborated on.

3.1 Phosphofructokinase

In the introduction, I mentioned the hypothesis of the periodicity of the insulin secretion of glucose-stimulated β -cells being due to oscillations in the glycolysis, which in turn may be due to product activation of PFK. In order to theoretically investigate this, a model of the flux-concentration relationship of muscle-type PFK, which is the PFK isozyme present in β -cells, is needed. Here, we will show that the GRH equation is adequate for describing the kinetics of muscle-type PFK.

PFK catalyzes the reaction



The enzyme is affected by many allosteric modifiers; it has well-characterized activating sites for AMP and fructose bisphosphates, as well as inhibitory sites for citrate and ATP [38]. As a source for experimental data on the kinetics of PFK, we used the study of Tornheim and Lowenstein [39]. In this study the effects of the modulators FBP, AMP and ATP on the kinetics were examined. Assuming a saturating concentration of ATP and a constant citrate concentration, the PFK GRH equation is written

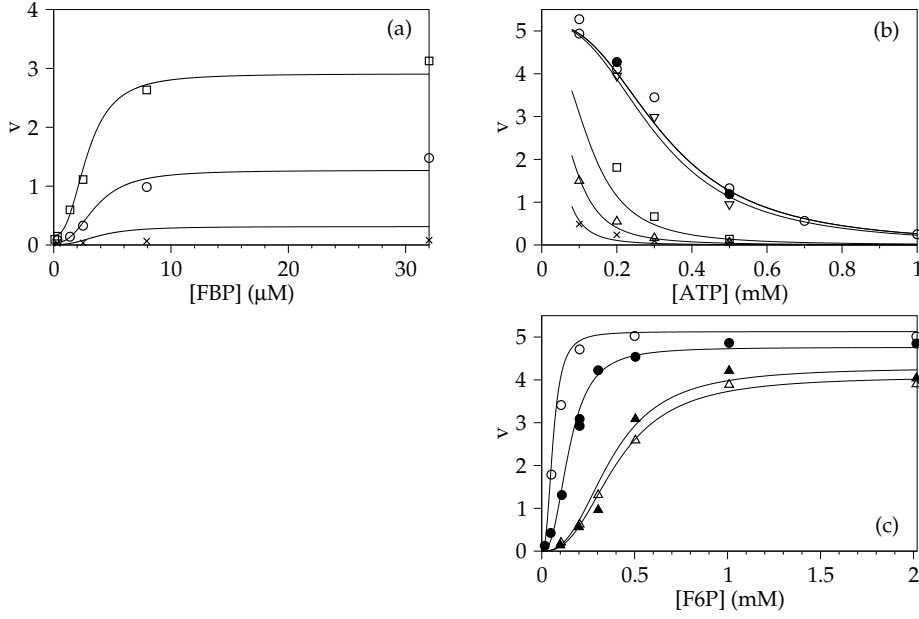


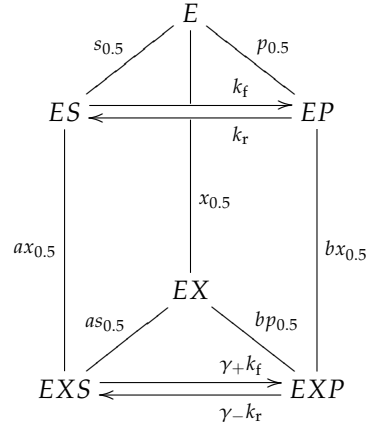
Figure 3.1: Experimental data of muscle PFK is indicated as follows: (a) AMP 50 μM , \circ AMP 20 μM , \times AMP 1 μM . (b) \triangle FBP 0.3 μM AMP 20 μM , FBP 1.4 μM AMP 20 μM , ∇ FBP 7.9 μM AMP 20 μM , \circ FBP 32 μM AMP 20 μM , \bullet FBP 84 μM AMP 20 μM , \times FBP 32 μM AMP. (c) \triangle ATP 0.2 mM AMP 1 μM FBP 32 μM , \circ ATP 0.2 mM AMP 20 μM FBP 32 μM , \bullet ATP 0.5 mM AMP 20 μM FBP 32 μM , \blacktriangle ATP 0.5 mM AMP 20 μM FBP 1.4 μM . Unless noted otherwise above or in the figures, concentrations were F6P 0.1 mM, ATP 0.5 mM, MgCl 8 mM. The reaction velocities v are in μM per minute. The solid lines are the corresponding theoretical curves calculated from equation . The optimized parameter set was $S_{0.5} = 0.26$ mM, $X_{\text{FBP}} = 4.1$ μM , $X_{\text{AMP}} = 39$ μM , $X_{\text{ATP}} = 0.034$ mM, $h = 2.6$, $\alpha_{\text{FBP}} = 30$, $\alpha_{\text{AMP}} = 880$, $\alpha_{\text{ATP}} = 8.8 \times 10^{-5}$, $\gamma_{\text{FBP}} = 1.4$, $\gamma_{\text{AMP}} = 1.3$, $\gamma_{\text{ATP}} = 0$, $V = 2.9$ $\mu\text{M}/\text{min}$.

$$v = \frac{\prod_i \frac{1 + \gamma_i \alpha_i \xi_i^h}{1 + \alpha_i \xi_i^h} V \sigma^h}{\sigma^h + \prod_i \frac{1 + \xi_i^h}{1 + \alpha_i \xi_i^h}}, \quad (3.1)$$

where $\sigma = \text{F6P}/S_{0.5}$, $\xi_i = [i]/X_i$ and where i may represent FBP, AMP or ATP. Flux is here denoted v ; in the following j will be used to indicate steady-state fluxes in multi-enzyme systems only.

Experimental data from the study of Tornheim and Lowenstein [39] were scanned manually and are given in figure 3.1 as symbols. The operationally well-defined parameters of the GRH equation makes it easy to come up with starting guesses for the parameters. Thus, one expects h , α_{FBP} , α_{AMP} , γ_{FBP} , and γ_{AMP} to be greater than one, while α_{ATP} and γ_{ATP} should be less than one. An optimization in least squares sense yielded the parameter set presented in caption of figure 3.1. In the figure, the solid lines are the rates calculated according to equation 3.1 using the optimized parameter set.

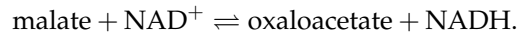
Figure 3.2: A model of a one-substrate one-product enzyme with a modifier X affecting the forward and backward catalytic rates differently.



The experimentally found rate can be seen to be quite well described by the GRH equation. Still, this equation has fewer parameters than any other equation that has earlier been used to describe muscle-type PFK (see **paper II**).

3.2 Malate Dehydrogenase

Ironically, shortly after having finished paper II, I was faced with the task of describing an enzyme whose behaviour definitely *cannot* be captured by the GRH equation. The enzyme malate dehydrogenase (MDH) is part of the TCA cycle and of the MA shuttle and catalyzes the reaction



Citrate acts upon the mitochondrial isozyme, MDHm, as an allosteric modifier, increasing the forward limiting rate V_f roughly with a factor three, while leaving the backward limiting rate V_r unchanged [40]. This behaviour is fundamentally alien to e.g. equation 2.13, which assumes that both V_f and V_r are modified by the same factor. As a first step towards a solution of this problem, consider a simple one-substrate, one-modifier enzyme acting according to the minimal scheme presented in figure 3.2.

We have here assumed that the modifier affects the forward and backward catalytic constants differently. When traversing the square formed by ES , EP , EXP , and EXS , detailed balance [41] implies that

$$\frac{\gamma_+}{\gamma_-} = \frac{a}{b} = \frac{\beta}{\alpha}.$$

Again using the method of Cha [33], we arrive at the rate equation

$$v = \frac{V(1 + \gamma_+ \alpha \xi) \sigma \left(1 - \frac{\Gamma}{K_{\text{eq}}}\right)}{1 + \xi + (1 + \alpha \xi) \sigma + (1 + \beta \xi) \pi}.$$

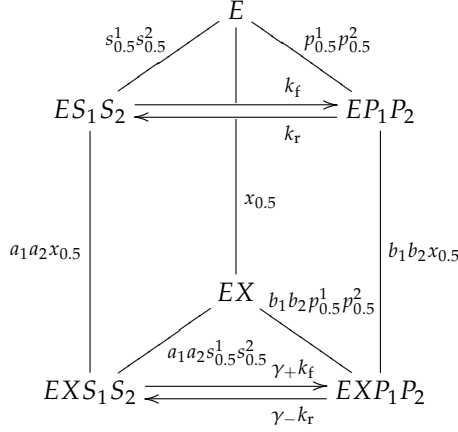


Figure 3.3: A model of a two-substrate two-product enzyme with a modifier X affecting the forward and backward catalytic rates differently.

Note that for the backward reaction, $\lim_{\xi \rightarrow \infty} \frac{1+\gamma+\alpha\xi}{1+\beta\xi} = \lim_{\xi \rightarrow \infty} \frac{1+\gamma-\beta\xi}{1+\beta\xi} = \gamma_-$. In fact, we have here derived a reversible version of the classical general modifier mechanism of Botts and Morales [42].

It is straightforward to extend this model to a two-substrate two-product enzyme, which has to be done in order to obtain an equation for MDHm. We now have two normalized substrate concentrations σ_1 and σ_2 , whose normalization constants (i.e. dissociation constant) are modified by factors α_1 and α_2 , respectively, when the modifier X is bound to the enzyme. We also have normalized product concentrations π_1 and π_2 together with factors β_1 and β_2 , and we assume that the dissociation constants are independent of the order by substrates and products bind to the enzyme. A simplified scheme representing this model is presented in figure 3.3. Detailed balance at equilibrium now yields:

$$\frac{\gamma_+}{\gamma_-} = \frac{\beta_1\beta_2}{\alpha_1\alpha_2} \quad (3.2)$$

and we arrive at the following rate equation:

$$v = \frac{V(1 + \gamma_+\alpha_1\alpha_2\xi)\sigma_1\sigma_2\left(1 - \frac{\Gamma}{K_{eq}}\right)}{\left[(1 + \alpha_1\xi)\sigma_1 + (1 + \alpha_2\xi)\sigma_2 + (1 + \beta_1\xi)\pi_1 + (1 + \beta_2\xi)\pi_2 + \xi_1(\alpha_1\sigma_1 + \beta_1\pi_1)(\alpha_2\sigma_2 + \beta_2\pi_2) + 1 + \xi + (\sigma_1 + \pi_1)(\sigma_2 + \pi_2)\right]} \quad (3.3)$$

Unfortunately, since the α s and β s may attain different values, there is no way to factorize the denominator as elegantly as we have done prior to this point. Be that as it may, how do we estimate the parameters of this equation? Consider an experimental situation where the amount of product is small enough to be neglected, i.e. $\pi_1 = \pi_2 = \Gamma = 0$. If we now invert equation 3.3 and collect the terms containing $1/\sigma_1$, we obtain

$$\frac{1}{v} = \frac{1}{\sigma_1} \times \frac{1 + \sigma_2 + \xi(1 + \alpha_2\sigma_2)}{V\sigma_2(1 + \gamma_+\alpha_1\alpha_2\xi)} + \frac{1 + \xi(\alpha_1 + \alpha_1\alpha_2\sigma_2)}{V\sigma_2(1 + \gamma_+\alpha_1\alpha_2\xi)}.$$

This equation is commonly used to estimate V and $s_{0.5}$ from double-reciprocal plots of $1/S_1$ vs. $1/v$. The situation is clearest if S_2 is present in a saturating amount, i.e. $\sigma_2 \rightarrow \infty$. Then, if $\xi = 0$,

$$\frac{1}{v} \rightarrow \frac{1}{\sigma_1} \times \frac{1}{V} + \frac{1}{V},$$

and if $\xi \rightarrow \infty$,

$$\frac{1}{v} \rightarrow \frac{1}{\gamma_+ \alpha_1 \sigma_1} \times \frac{1}{V} + \frac{1}{\gamma_+ V}. \quad (3.4)$$

Thus, from two double-reciprocal plots made under these conditions, it is possible to obtain V , $S_{0.5}^1$, γ_+ and α_1 from the slopes and intersections with the $1/v$ -axis.

We now turn to the kinetics of MDHm. We let 1 represent the malate-oxaloacetate substrate-product pair and 2 represent the NAD^+ -NADH substrate-product pair. The modifier X is of course citrate. The constant γ_+ represents the factor by which citrate increases the forward limiting rate and as noted earlier, $\gamma_+ \approx 3$. There is also a factor γ_{1-} representing the factor by which citrate increases the backwards limiting rate, and which, since citrate does not affect the backwards limiting rate, is equal to one. But is the detailed balance condition 3.2 satisfied? The data of Gelpí et al. [40] suggest that citrate increases the product half-activation point for NADH roughly by a factor ten, i.e. $\beta_2 \approx 0.1$. The product half-activation point for oxaloacetate appears unaffected, thus $\beta_1 \approx 1$. These investigators further noted that citrate may act both as an activator and as an inhibitor in the forward reaction, depending on the NAD^+ concentration. The catalytic constant of the enzyme is certainly increased, but at the same time, the half-activation point with respect to NAD^+ is increased roughly by a factor three – i.e. $\alpha_2 \approx 0.1$ (cf. equation 3.4). Remarkably, the data of Gelpí et al. [40] suggest that $\alpha_1 \approx 0.3$ which is compatible with equation 3.2. Thus, the simple scheme of figure 3.3 indeed seems to be roughly compatible with the kinetics of MDHm. I let equation 3.3 reproduce figure 4b in the study of Gelpí et al. [40] and present the results in figure 3.4. The reader should note the two distinct regions in the $1/\text{NAD}^+$ -dimension where citrate either inhibits or activates. The regions are separated by an intersection point where the rate is insensitive to citrate. This point may in the case of saturating concentrations of malate be determined by taking the derivative

$$\frac{d\left(\frac{1}{v}\right)}{d\xi} = \frac{1 + \alpha_1 \sigma_1 + \alpha_2 \sigma_2 + \alpha_1 \alpha_2 \sigma_1 \sigma_2 - \gamma_+ \alpha_1 \alpha_2 (1 + \sigma_1 + \sigma_2 + \sigma_1 \sigma_2)}{V \sigma_2 (1 + \gamma_+ \alpha_1 \alpha_2 \xi)^2},$$

which vanishes for all values of ξ if

$$\sigma_2 = \frac{1 + \alpha_1 \sigma_1 - \gamma_+ \alpha_1 \alpha_2 (1 + \sigma_1)}{\gamma_+ \alpha_1 \alpha_2 (1 + \sigma_1) - \alpha_2 - \alpha_1 \alpha_2 \sigma_1}.$$

As $\sigma_1 \rightarrow \infty$, this equation produces a positive (i.e. physical) σ_2 only when

$$\frac{\gamma_+ - 1}{1 - \gamma_+ \alpha_2} > 0,$$

which then is the condition determining whether the modifier is able to act both as an inhibitor and as an activator.

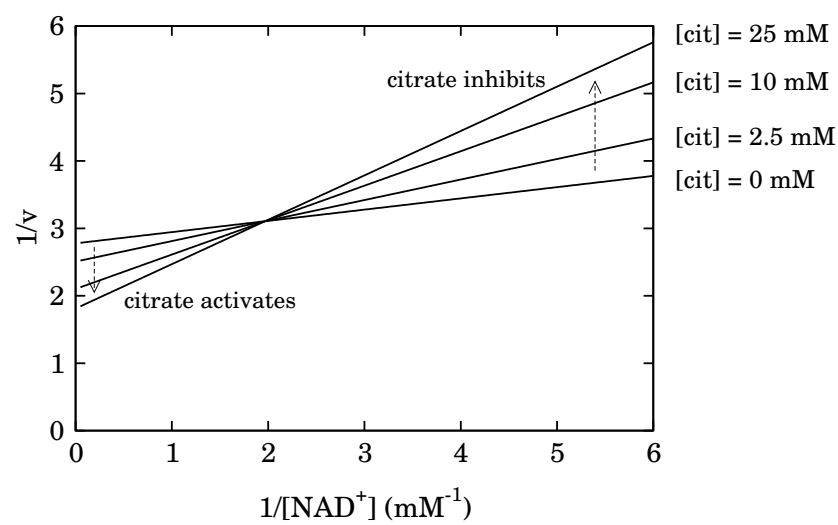


Figure 3.4: **Reproduction of the experimental data presented in figure 4b in the study of Gelpí et al. [40].** We see in this double-reciprocal Lineweaver-Burk plot that citrate activates MDH at high NAD^+ levels, but inhibit MDH at low NAD^+ levels. Malate is here constant at 10 mM and no products are assumed to be present. Parameters used: $V_{\text{MDHm}} = 0.36 \mu\text{M}/\text{min}$, $S_{0.5}^{\text{malate}} = 3 \text{ mM}$, $S_{0.5}^{\text{NAD}} = 0.06 \text{ mM}$, $X_{0.5}^{\text{citrate}} = 0.9 \text{ mM}$, $\alpha_{\text{malate}} = 0.3$, $\alpha_{\text{NAD}} = 0.1$, and $\gamma_+ = 3$.

Chapter 4

Theory: From the Parts to the Whole. Modeling, Analysis and Simulation of Biochemical Reaction Systems

We will now consider networks of biochemical reactions. We will primarily consider reactions taking place between different species in the cytosol, and start with the hypothesis of an isotropic (“well-stirred”) cell. When formulating a model to use for simulating any real world system, it is practical to try to formulate an abstraction of the features of this system, to facilitate the model construction. When considering a set of biochemical reactions in a living cell, an attempt to such a formulation could be to consider the reactions to comprise a network, or graph, with:

- **Pools of species**, nodes in the graph, which are here denoted with the vector of metabolites $\mathbf{x} = (x_1, x_2, \dots)^T$ (unit: mM).
- **Reactions or fluxes** denoted $(v_1, v_2, \dots)^T = \mathbf{v}$ (unit: mM/s) between these species, which can be considered as arrows or directed edges between nodes. Steady-state fluxes are denoted $(j_1, j_2, \dots)^T = \mathbf{j}$. We will usually consider each flux as catalyzed by one enzyme and the rate given by a suitable rate equation, which often is a function of the concentration of the enzyme’s substrates and products. Further, species other than the substrates and products of an enzyme may modulate its catalytic rate.

The fluxes may be translated to derivatives by the elementary linear transformation

$$\dot{\mathbf{x}} = \mathbf{N}\mathbf{v}, \quad (4.1)$$

where \mathbf{N} denotes the stoichiometric matrix. The network’s behavior over time may be obtained by integrating this system of (usually) nonlinear ODEs.

4.1 Critical Assumptions

The ansatz for a description of the cellular metabolism, or part thereof, that is described above is dependent on several critical assumptions and simplifications that are often implicit in the literature of metabolic modeling. I suggest five of the, to my mind, most important of these assumptions below. The reader is certainly encouraged to question these assumptions and their justifications as I have often done myself.

1. In cellular metabolism, enzyme catalyzed biochemical reactions are generally not considered to be diffusion controlled [43], i.e. diffusion occur on a much faster time scale than the reactions. Thus, any spatial inhomogeneities in a cellular compartment may in a limit sense considered to be evened out before any reactions modify the chemical composition of it. This justifies the use of the “well-stirred cell” approximation made above.
2. I have ignored the intrinsic fluctuations in reaction rates and concentration of species, which are due to the stochastic nature of biochemical reactions [27]. Fluctuations must be considered when the concentrations are so low that the averages of the number of molecules are not representative because of broad and skewed non-Poissonian probability distributions. However, the β -cell volume is in the order of pl [44]. The metabolites considered in this thesis are usually present in concentrations at least in the order of μM , corresponding to at least about 10^5 molecules per cell which is a regime that should justify a deterministic description. Still, fluctuations may be significant when the system is not asymptotically stable in the continuous macroscopic description (for instance at a Hopf bifurcation, see section 4.4) [27]. However, I have investigated systems in asymptotically stable regimes, which justifies a deterministic continuous description.
3. The metabolites of the central β -cell metabolism considered in this thesis are much smaller than the enzymes that catalyze the biochemical reactions. This justifies not considering effects of so-called macromolecular crowding [45], which limits the diffusion of large molecules.
4. I have not considered the possible biochemical effect of *metabolite channeling* which is proposed to occur in parts of the glycolysis and TCA cycle. Metabolite channeling is thought to occur when two or more enzymes, catalyzing two or more reactions occurring in chain, associate and channel the product of the first enzyme in the chain directly to the next enzyme, without letting the metabolite diffuse via the cytosol. The effect of metabolite channeling on overall reaction rates is probably marginal in most cases [37].
5. A potentially serious issue is the question whether the quasi-steady-state assumption made when deriving the enzyme rate equations (see section 2.2) really is justifiable for an *in vivo* situation. The question has recently been addressed both for global steady state conditions [46] and for periodic influxes [47] to networks of enzyme catalyzed reactions. These

investigations revealed that the errors stemming from the quasi-steady-state assumption are not necessarily significant even when the assumption is not strictly valid, for example when the system is oscillatory. I have focused more on principles than on the *exact* replication of experimental observations, hence I have not pursued this matter further.

4.2 Metabolic Control Analysis (MCA)

As in other natural sciences, sensitivity analysis provides important insights into biochemical regulatory networks. The approach to sensitivity analysis for biochemical systems used in this thesis is termed Metabolic Control Analysis (MCA). On a basic level, MCA is a framework concerning steady-state fluxes \mathbf{j} and concentrations as functions, putting the derivatives of these functions with respect to enzyme concentrations into the center stage as control coefficients.

The subject of MCA is covered in excellent textbooks [48, 49], and it is not possible to give a thorough introduction to the subject on these few pages. Instead, I will compactly describe one particular approach to MCA introduced by Reder [50] which was used in **paper V** and in the analysis in section 5.2. Here, only steady-state solutions to equation 4.1, i.e. concentrations \mathbf{x} such that $\mathbf{N}\mathbf{j} = 0$, are considered, although during the last couple of years MCA has been extended to non-steady-state as well as spatially heterogeneous systems too [51, 52].

First, let \mathbf{L} be the link matrix, used to decompose the stoichiometry matrix in order to remove linear dependencies between its rows so that

$$\mathbf{N} = \mathbf{L}\bar{\mathbf{N}},$$

where $\bar{\mathbf{N}}$ has full rank and where \mathbf{L} is the identity matrix if \mathbf{N} has full rank. Let \mathbf{D} be the matrix of unscaled elasticities

$$\mathbf{D} = \frac{\partial \mathbf{v}}{\partial \mathbf{x}}.$$

We now take interest in the steady-state solutions to $\mathbf{N}\mathbf{v} = \dot{\mathbf{x}}$. We may, via implicit partial differentiation and using the steady-state condition $\mathbf{N}\mathbf{j} = 0$, calculate the control matrices

$$\begin{aligned} \mathbf{C}^{\mathbf{x}} &= \left(\frac{\partial \mathbf{x}}{\partial \mathbf{p}} \right) \left(\frac{\partial \mathbf{v}}{\partial \mathbf{p}} \right)^{-1} = -\mathbf{L} (\bar{\mathbf{N}}\mathbf{D}\mathbf{L})^{-1} \bar{\mathbf{N}} \\ \mathbf{C}^{\mathbf{j}} &= \left(\frac{\partial \mathbf{j}}{\partial \mathbf{p}} \right) \left(\frac{\partial \mathbf{v}}{\partial \mathbf{p}} \right)^{-1} = \mathbf{I} - \mathbf{D}\mathbf{L} (\bar{\mathbf{N}}\mathbf{D}\mathbf{L})^{-1} \bar{\mathbf{N}}. \end{aligned} \quad (4.2)$$

Here, \mathbf{I} is the identity matrix and \mathbf{p} is a vector of parameters so that $\partial \mathbf{v} / \partial \mathbf{p}$ is square and non-singular. $\mathbf{C}^{\mathbf{x}}$ is the concentration control matrix and $\mathbf{C}^{\mathbf{j}}$ is the flux control matrix. These matrices tell us how strong control each enzyme has over each steady-state concentration and flux. Even more, these systemic properties are expressed solely in terms of local properties, i.e. the components of \mathbf{D} , which only contains partial derivatives of the different rate equations with respect to the concentrations.

4.3 The Method of Numerical Continuation

Much of the work in the thesis concerns how steady-state solutions to equation 4.1 vary with different parameters, e.g. enzyme activities. Mathematically, this means investigating solutions \mathbf{x} to

$$\mathbf{Nj}(\mathbf{x}, \lambda) = 0 \quad (4.3)$$

as a function of the parameter λ . This is usually only feasible using numerical methods.

A brute-force method to compute solutions to equation 4.3 would be to just vary λ and successively compute solutions using standard Newton methods for solving nonlinear equations. This is however unnecessary time-consuming. We may view equation 4.3 as a function $F(x) : \mathbf{R}^{n+1} \rightarrow \mathbf{R}^n$, where $F(x) = \mathbf{Nj}(x)$ and $x = (\mathbf{x}^T, \lambda)^T$. The brute force method may be viewed as a predictor-corrector method, which makes the stupid choice of making predictions only in the λ direction. A better method is Moore-Penrose continuation [53]. This algorithm allows us to make predictions in any direction, which significantly speeds up the calculations if the solutions \mathbf{x} do not vary much with λ .

1. *Prediction.* Given a point x_k on the solution curve and a tangent vector v_k to the curve at this point, make a first prediction X^0 :

$$X^0 = x_k + hv_k,$$

where h is a stepsize that needs to be sufficiently small and may be changed during the course of several iterations.

2. *Correction.* Since the Jacobian $J(X)$ of $F(X)$ is not square, we have to add an equation in order to be able to use Newton iterations to find a point x_{k+1} on the solution curve. We choose to aim for the point closest to the point X^0 , making the vector $(x_{k+1} - X^0)$ orthogonal to the tangent vector v_{k+1} to the solution curve at the point x_{k+1} . This is our additional equation, and we now have:

$$\begin{aligned} F(x_{k+1}) &= 0 \\ v_{k+1}^T (x_{k+1} - X^0) &= 0. \end{aligned}$$

Now, starting with a first estimation $V^0 = v_k$ of v_{k+1} , a Newton algorithm solving this problem for sufficiently small h is

$$\begin{aligned} X^{k+1} &= X^k - H_x^{-1}(X^k, V^k) H(X^k, V^k) \\ V^{k+1} &= V^k - H_x^{-1}(X^k, V^k) R(X^k, V^k), \end{aligned}$$

where $H(X, V) = \begin{pmatrix} F(X) \\ 0 \end{pmatrix}$, $H_x(X, V) = \begin{pmatrix} J(X) \\ V^T \end{pmatrix}$ and $R(X, V) = \begin{pmatrix} J(X)V \\ 0 \end{pmatrix}$.

The *stability* of the steady-state solutions represented by the solution curve of equation 4.3 is of critical interest, which is the subject I address next.

4.4 More Complex Behavior: from Steady State to Prolonged Oscillations

Mathematically, a steady-state solution to 4.1 is a fixpoint of the ODE system. According to the principle of linearized stability, the stability of a fixpoint may be determined via the eigenvalues of the Jacobian \mathcal{J} . If the real parts of all eigenvalues are negative, the fixpoint is *stable* in the sense that all solutions in a neighbourhood of it converge to it as $t \rightarrow \infty$. Otherwise, it is *unstable* and all solutions in a neighbourhood of it diverge from it. In the particular case of a two-dimensional system, the stability is quite simple to analyze, and one arrives at the classification summarized in table 4.1.

In two-dimensional systems where the solutions are bounded inside a region of the two-dimensional state space, periodic solutions or limit cycles may exist. If the bounded region only contains repellers, the Poincaré-Bendixson Theorem [54] dictates that the solutions converge towards a limit cycle as $t \rightarrow \infty$. Therefore, when searching for periodic solutions to a two-dimensional system, the investigation of the stability of fixpoints is important. In **paper I**, these principles were made use of when analyzing the stability properties of the glycolysis in the β -cell. There it is shown that the steady-state solution to a model of β -cell glycolysis undergoes a transition from a spiral node to a spiral repeller — this transition is a so-called Hopf bifurcation — as the glucose concentration is raised from a low value to a higher value.

Table 4.1: **The stability of a fixpoint of a two-dimensional dynamical system.** There are six cases (excluding borderline cases), which are determined by the trace of the Jacobian, $\text{Tr}\mathcal{J}$, and by the determinant of the Jacobian, Δ .

	$\text{Tr}\mathcal{J} < 0$	$\text{Tr}\mathcal{J} > 0$
$\Delta > \frac{1}{4} (\text{Tr}\mathcal{J})^2$	spiral node	spiral repellor
$0 < \Delta < \frac{1}{4} (\text{Tr}\mathcal{J})^2$	node	repellor
$\Delta < 0$	saddle point	saddle point

Chapter 5

Application: The Glycolysis, NADH Shuttles and TCA Cycle

5.1 The Glycolysis

The glycolysis has a very crucial role in the GSIS of the β -cell and was therefore chosen as an object for my theoretical investigations (**paper I**). This pathway, ancient and ubiquitous in the biosphere as it is, operates just as in any cell type or organism, seen just to the sequence of reactions and to the stoichiometry: per one molecule entering the glycolysis, two molecules of pyruvate comes out, along with two molecules ATP and NADH (of course ignoring pesky complications like the pentose phosphate shunt, but the activity of this pathway seems to be low in the β -cell [55]). However, when looking into the kinetic peculiarities, two special traits of the set of isozymes in the β -cell grant its glycolysis a unique kinetic profile:

1. The hexokinase isozyme is type IV, usually called *glucokinase* (GK).
2. The phosphofructokinase isozyme is the muscle type (M-type).

The first trait has for 35 years motivated β -cell investigators to identify GK as *the glucose sensor* of the β -cell [56]. The reasons for this is twofold; first, the reaction is at physiological levels of metabolites nearly irreversible (since it consumes ATP, the reader may verify this by consulting thermodynamical tables [28, 29, 30] along with data on metabolite levels [57, 58]). There does not seem to be any significant product inhibition of the reaction [56]. In a linear pathway with an irreversible first step without product inhibition, this step solely determines the steady-state flux through the pathway. This is very unusual but appears to be the case in the β -cell. Second, the $S_{0.5}$ for glucose is 5–10 mM, which is just around the physiological glucose concentration, and the concentration-rate curve is sigmoidal with a Hill coefficient just below 2 [56]. Thus, GK, and ultimately the glycolytic rate, seems to be optimized to have its rate quite tightly controlled by glucose. Keeping things simple and

straightforward, I write

$$v_{\text{GK}} = \frac{V_{\text{GK}} \sigma^{h_{\text{GK}}}}{1 + \sigma^{h_{\text{GK}}}},$$

where $\sigma = [\text{glucose}]/S_{0.5}^{\text{GK}}$.

The second trait gives the glycolysis in the β -cell an ability to oscillate. Oscillations in glycolysis have been demonstrated in several organisms and model systems of which yeast is the most well-studied and the oscillations in all systems have been attributed as due to autocatalysis of PFK [59, 60, 61]. The time scale of glycolytic oscillations is typically in the range of minutes, which has prompted the hypothesis that they might be the mechanism behind the pulsatile insulin secretion. During the last decade, indications of an oscillatory glycolysis in the β -cell have accumulated, with observations of oscillations in cytosolic NAD(P)H concentration, oxygen consumption, glucose-6-phosphate concentration and the ATP/ADP ratio [62, 63, 64, 65, 66, 67, 68, 69]. Importantly, the oscillations of the latter parameter correlates with insulin secretion and $[\text{Ca}^{2+}]_i$ [70]. Therefore, a minimal hypothesis is that the glycolytic oscillations are due to the autocatalysis of the PFK reaction [16, 70], and further, that this is the cause of slow bursting and corresponding insulin secretion. Clinically, it has been shown that an inherited PFK deficiency results in loss of the oscillations of insulin secretion [71], which motivates thorough investigations of the role of PFK in the β -cell. Here, I ask the reader to ponder the discussion in the introduction, regarding the enzyme that is activated by its product and may cause the system that it is a part of to oscillate, or the system might attain a steady-state. Soon, the time has come to do the mathematical analysis of this system, but first, I give a rate equation for PFK:

$$v_{\text{PFK}} = \frac{V_{\text{PFK}} \sigma^{h_{\text{PFK}}}}{\sigma^{h_{\text{PFK}}} + \frac{1 + (q\pi)^{h_{\text{PFK}}}}{1 + \alpha(q\pi)^{h_{\text{PFK}}}}}.$$

Here, $\sigma = [\text{F6P}]/S_{0.5}^{\text{PFK}}$, $\pi = [\text{FBP}]/S_{0.5}^{\text{FBA}}$ and $q = S_{0.5}^{\text{FBA}}/X_{0.5}^{\text{FBA}}$. Again I have kept things as simple as possible and have hence ignored the slight increase of the effective limiting rate of the product/modifier FBP. Note that this equation is valid only in the limit of nearly constant ATP and AMP levels – it is thus an even simpler equation than that presented in **paper II**.

The time is now ripe to set up a minimal model of β -cell glycolysis, and we will here follow the construction path of the simplest of the two models presented in **paper I**. The activities of the different enzymes in the β -cell glycolysis have been measured in two studies [72, 73] and the activities of glucose-6-phosphate isomerase (GPI) and the enzymes downstream of fructose-bisphosphate aldolase (FBA) were found to have at least an order of magnitude higher activities than this enzyme. This motivates a minimal model based on the scheme in figure 5.1. Assuming that the FBA rate may be approximated by a simple rate equation of Michaelis-Menten form:

$$v_{\text{FBA}} = \frac{V_{\text{FBA}} \pi}{1 + \pi},$$

the scheme in figure 5.1 may be translated to an ODE system accordingly:

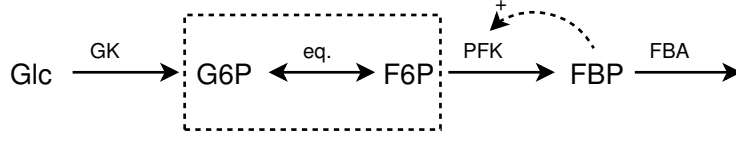


Figure 5.1: **A core model of β -cell glycolysis.** The dashed box surrounds metabolites considered to be in pseudo-equilibrium. The dashed arrow indicates the positive feed-back elicited by the PFK product FBP. In the simplest case presented here, the removal of mass from the glycolysis is controlled solely by FBA.

$$\begin{aligned}\dot{\sigma} &= \frac{f}{S_{0.5}^{\text{PFK}}} (v_{\text{GK}} - v_{\text{PFK}}) \\ \dot{\pi} &= \frac{1}{S_{0.5}^{\text{FBA}}} (v_{\text{PFK}} - v_{\text{FBA}}),\end{aligned}\quad (5.1)$$

The glucose-6-phosphate isomerase (GPI) catalyzed reaction has been assumed to be in quasi-equilibrium with an equilibrium constant $K_{\text{eq}}^{\text{GPI}} = [\text{F6P}]/[\text{G6P}]$ which enters the expression $f = K_{\text{eq}}^{\text{GPI}}/(1 + K_{\text{eq}}^{\text{GPI}})$. It is now of interest to calculate the steady-state solutions of the ODE system 5.1 and to investigate the possibility of an unstable steady-state. An unstable steady-state sets the scene for periodic limit-cycle solutions to 5.1, which, as may be realized from the discussion above, are of greatest interest. Let us immediately assess the stabilities of the fixpoints of equation 5.1. We may write the Jacobian \mathcal{J} accordingly:

$$\mathcal{J} = \begin{pmatrix} -k_1 \frac{\partial v_{\text{PFK}}}{\partial \sigma} & -k_1 \frac{\partial v_{\text{PFK}}}{\partial \pi} \\ k_2 \frac{\partial v_{\text{PFK}}}{\partial \sigma} & k_2 \left(\frac{\partial v_{\text{PFK}}}{\partial \pi} - \frac{\partial v_{\text{FBA}}}{\partial \pi} \right) \end{pmatrix}$$

where $k_1 = f/S_{0.5}^{\text{PFK}}$ and $k_2 = 1/S_{0.5}^{\text{FBA}}$. We now consult table 4.1 to find out what can be said. We find out that $\Delta > 0$ and thus a fixpoint will not be a saddle-point; it may only be a repellor or node. Which one is determined by the trace:

$$\text{Tr} \mathcal{J} = k_2 \left(\frac{\partial v_{\text{PFK}}}{\partial \pi} - \frac{\partial v_{\text{FBA}}}{\partial \pi} \right) - k_1 \frac{\partial v_{\text{PFK}}}{\partial \sigma}.$$

This expression explicitly states that *the activation of PFK by its product, i.e. a positive $\frac{\partial v_{\text{PFK}}}{\partial \pi}$, may yield an unstable steady-state of the system.* The stability is lost when the expression in the parentheses becomes sufficiently positive. It is here pertinent to remind the reader that such product activation of β -cell PFK has been directly measured [74]. The fixpoint(s) of the system 5.1 are located where the nullclines of the system, given by the two curves $\dot{\sigma} = 0$ and $\dot{\pi} = 0$, intersect in the (σ, π) plane. Glucose concentration alters only the $\dot{\sigma} = 0$ nullcline. As shown in **paper I**, the following holds on the $\dot{\pi} = 0$ nullcline:

$$\frac{d\sigma}{d\pi} = - \left(\frac{\partial v_{\text{PFK}}}{\partial \pi} - \frac{\partial v_{\text{FBA}}}{\partial \pi} \right) / \frac{\partial v_{\text{PFK}}}{\partial \sigma}.$$

Thus, the slope of the $\dot{\pi} = 0$ nullcline has to be sufficiently negative at the fixpoint in order for it to be unstable.

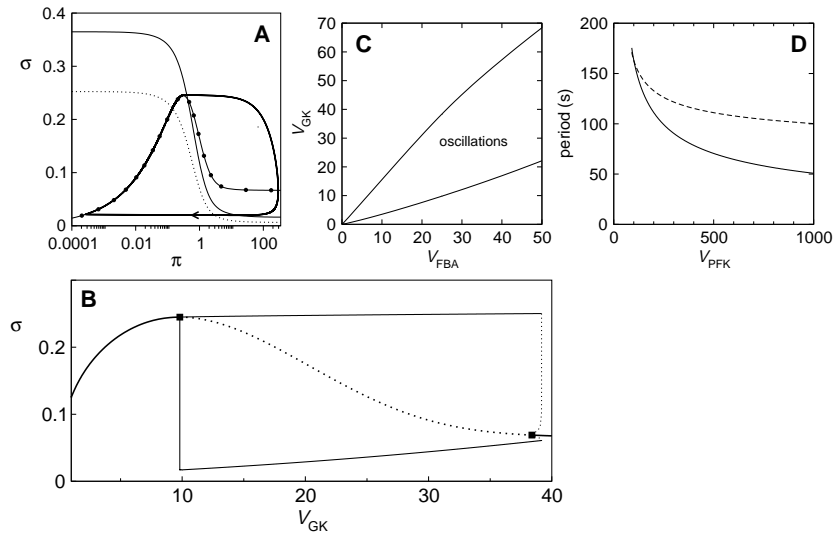


Figure 5.2: **The glycolysis model represented by the ODE system (5.1)** was solved using the following parameters: [glucose]= 10 mM; $V_{GK} = 10$ U/min, $V_{PFK} = 100$ U/min, $V_{FBA} = 25$ U/min; $S_{0.5}^{GK} = 8$ mM, $S_{0.5}^{PFK} = 4$ mM, $S_{0.5}^{FBA} = 5$ μ M; $K_{eq}^{GPI} = 0.3$, $h_{GK} = 1.7$, $h_{PFK} = 2.5 - 1.5q\pi/(1 + q\pi)$, $\alpha_{PFK} = 5^{h_{PFK}}$, $q = 0.5$. Tissue concentrations (U) were converted to mM by dividing with a factor of 180. (a). The time course of the solution of system (5.1). The solid and dotted lines represent σ and π , respectively. (b). Two-dimensional bifurcation diagram with V_{GK} and V_{FBA} as bifurcation parameters. (c). Dependence of the oscillation period on V_{PFK} . The dashed line was obtained when taking into account the equilibrium between different polymeric forms of PFK.

It is now time for numerical investigations of the system, its nullclines and fixpoints. Numerical values for the parameters of the rate equations were inferred via an extensive literature survey and are given in the legend of figure 5.2. The nullclines were computed and are shown in figure 5.2A. The $\dot{\sigma} = 0$ nullcline is translated as the glucose concentration is raised (dotted to solid curve). At the intersection with the $\dot{\pi} = 0$ nullcline (curve with circles) lies the fixpoint. It is stable for low glucose concentrations (dotted curve) but becomes unstable for higher glucose concentrations (solid curve, the intersection is on an interval where the slope of the $\dot{\pi} = 0$ nullcline is negative). Here, a stable limit cycle has appeared (thick solid closed curve).

Another view of the situation is presented in figure 5.2B. This diagram shows the steady-state (in the variable σ) as a function of the activity of GK. The curve was calculated using Moore-Penrose continuation. The thicker part of the curve represents a stable steady-state which becomes unstable at the filled square. The dotted part of the curve represents an unstable steady-state, which at very high GK activities again becomes stable. At the filled square, a limit cycle is born. This limit cycle, marked as the upper and lower limits of the periodic variations in σ with thin solid curves, persists throughout the region where the steady-state is unstable. The squares represent Hopf bifurcations. It is of interest to investigate how the Hopf bifurcations are affected by varia-

tions in different enzyme activities. This may yield predictions of how different experimental model systems and genotypes may behave with respect to glycolytic oscillations. In figure 5.2C, the locations of the Hopf bifurcations in the $(v_{\text{FBA}}, v_{\text{GK}})$ plane are plotted. It is evident that both GK and FBA exert control over this region. This prediction was new and may have significance in the understanding of β -cell glycolytic oscillations. It was found that PFK does not have any significant control over the locations of the bifurcations. On the other hand, V_{PFK} does influence the oscillation period, as seen in figure 5.2D. The dashed line was calculated also taking into consideration the fact that altering V_{PFK} probably also alters the distribution between different oligomeric forms of PFK. The solid line was calculated while not taking this into consideration. The results indicate that the equilibria between different oligomeric forms stabilizes the oscillation frequency with respect to perturbations and fluctuations in the concentration of the enzyme.

In summary, the minimal model of the β -cell glycolysis presented in **paper I** strengthens the hypothesis that glycolytic oscillations occur. It also gives experimentally testable predictions concerning the control of the occurrence and frequency of these oscillations.

5.2 NADH Shuttles and TCA Cycle

The study in **paper I** raised important questions on how to proceed with the modeling enterprise. The glycolysis was studied as an isolated module. In reality, this module is coupled to the rest of the cellular metabolism — not least to mitochondrial ATP production. In fact, the hypothesis of the glycolysis as a generator of the minute scale oscillations in insulin secretion is critically dependent on the assumption that glycolytic oscillations spur oscillations in the ATP/ADP ratio. We hence chose to boldly proceed in a direction where no theoretical investigator had gone before — to study the coupling of the glycolysis to the mitochondrial metabolism (**paper IV**). When doing so, it became natural also to investigate how glycolytic flux affects the putative GSIS coupling signals other than the ATP/ADP ratio: NADPH, malonyl-CoA and glutamate. A word of warning: this section by necessity contains a lot of abbreviations of enzyme names. The abbreviations are defined in the text and can also be found in the table of abbreviations in the preamble, as well as in **paper IV**.

The glycolytic flux is coupled to the mitochondrial metabolism via:

- Charge transfer: the GPDH reaction produces cytosolic NADH. The NADH is shuttled to the mitochondria via the glycerol-3-phosphate dehydrogenase (G3DH) and malate-aspartate (MA) shuttles.
- Carbon transfer: glycolytically produced pyruvate is transported into the mitochondria, where it is further metabolized in the TCA cycle.

The β -cell has some peculiar traits also in this part of the cellular metabolism: pyruvate is not only decarboxylated via pyruvate dehydrogenase (PDH), but also *carboxylated* via pyruvate carboxylase (PC). This *anaplerosis* has to be counterbalanced by *cataplerosis* – reactions that remove carbon from the metabolite pool of the TCA cycle. One such reaction is in the β -cell the reaction catalyzed

by ME, which produces the putative coupling factor NADPH. Another candidate is the reaction catalyzed by GDH, which, depending on the direction of the reaction, may produce the putative coupling factor glutamate. An overview of the mitochondrial metabolism is presented in figure 5.3. The coupling between the glycolysis and the mitochondrial metabolism was addressed by Eto et al. [75] in a thorough study. The authors showed that the two NADH shuttles constitute a redundant system. The blocking of either one of the shuttles (the G3DH shuttle was blocked via a knock-out of G3DH and the MA shuttle was blocked via inhibition of amino aspartate transaminase (AAT)) did not produce any significant effect, while the blocking of both shuttles did reduce the TCA cycle flux at the level of isocitrate dehydrogenase (IDH) and 2-oxoglutarate dehydrogenase (OGDH) by about 50%. At the same time the glycolytic rate remained unchanged. Since the shuttles were blocked, the authors argued, the glycolytically produced NADH had to be reoxidized by an unknown factor. A candidate is lactate dehydrogenase (LDH), but this enzyme seems to have a low activity in β -cells. An overview of the reaction network we studied is given in figure 5.3. We represented this reaction network by the following ODE system:

$$\begin{aligned}
\dot{x}_1 &= f_1 \times (v_{CS} - v_{IDHm} - v_{IDHPm} - c \times v_{IDHPc} - c \times v_{ACS}) / S_{IDHm}^1 \\
\dot{x}_2 &= f_2 \times (v_{IDHm} + v_{IDHPm} + c \times v_{IDHPc} - v_{OGDH} - c \times v_{AATc} - \\
&\quad - v_{AATm} - v_{GDH}^8 - v_{GDH}^{10}) / S_{OGDH}^2 \\
\dot{x}_3 &= f_3 \times (v_{OGDH} - v_{MDHm} - c \times v_{MDHc} - c \times v_{ME}) / S_{MDHm}^3 \\
\dot{x}_4 &= (v_{PC} + v_{MDHm} + v_{AATm} - v_{CS}) / S_{CS}^4 \\
\dot{x}_5 &= (v_{AATc} + v_{MDHc} + v_{ACS}) / P_{MDHc}^5 \\
\dot{x}_6 &= f_6 \times (c \times v_{GPDH} + c \times v_{ME} - c \times v_{LDH} - v_{PDH} - v_{PC}) / S_{PDH}^6 \\
\dot{x}_7 &= (v_{CS} - v_{PDH} - v_{FO}) / [CoA]_{tot} \\
\dot{x}_8 &= (v_{resp} + v_{GDH}^8 - v_{PDH} - v_{FO} - v_{IDHm} - v_{OGDH} - \\
&\quad - v_{MDHm}) / [NADHm]_{tot} \\
\dot{x}_9 &= (v_{G3DH} - v_{MDHc} - v_{GPDH}) / [NADHc]_{tot} \\
\dot{x}_{10} &= (v_{GDH}^{10} - v_{IDHPm}) / [NADP]_{tot} .
\end{aligned}$$

The factor c is the ratio between the volumes of the cytosolic and mitochondrial compartments (≈ 20). The different factors f_i follow from the quasi-equilibria that are assumed in the model, which are described in detail in the appendix in **paper IV**. Also, the different rate equations are given in the appendix of this paper. The rate equations were derived according to the principles outlined in chapter 2.2, where also the rate equation for MDH is discussed in detail. The parameters were inferred from an extensive literature survey (see **paper IV** for references). This system was analyzed in terms its steady-state solutions, i.e.

$$\begin{aligned}
\dot{x}_1 &= 0 \\
&\vdots \\
\dot{x}_{10} &= 0.
\end{aligned} \tag{5.2}$$

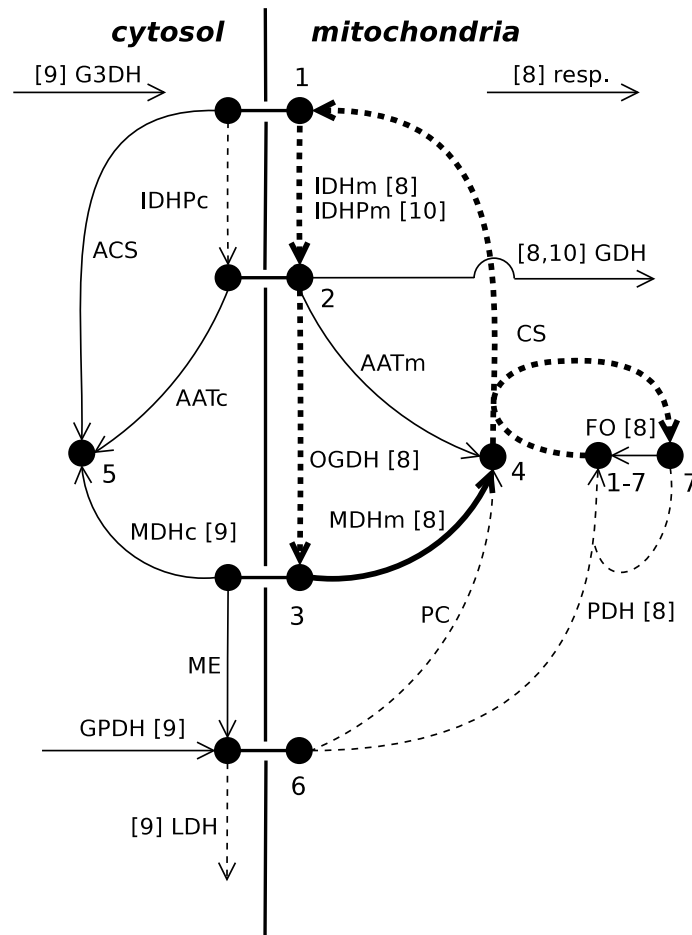


Figure 5.3: **The model studied in paper IV.** The numbers refer to metabolites: 1, isocitrate; 2, 2-oxoglutarate; 3, malate; 4, mitochondrial oxaloacetate; 5, cytosolic oxaloacetate; 6, pyruvate; 7, CoA; 1-7, acetyl-CoA; 8, mitochondrial NAD(H); 9, cytosolic NAD(H); 10, mitochondrial NADP(H). The reactions are represented as arrows. The corresponding enzymes are written with standard abbreviations, see the preamble and **paper IV** for a table of these. A bracketed number (e.g. [8]) after an enzyme abbreviation indicates that the reaction produces NAD(P)H, a bracketed number before the abbreviation indicates that the reaction consumes NAD(P)H. Dashed arrows represent irreversible enzymes, solid arrows represent reversible enzymes. The thicker arrows represent the reactions of the classical TCA cycle. Metabolites transported between the mitochondrial and cytosolic compartments are assumed to do so quickly, so that these transport processes may be approximated by their thermodynamic equilibrium condition.

We also define the *gain*, denoted γ , as

$$\gamma_x = \frac{\Delta x}{x},$$

which represents the change in the steady-state level of an output signal x (a steady-state flux or concentration) in response to a raised glycolytic flux V_{GPDH} , usually from 0.005 mM/s to 0.015 mM/s.

The first question we addressed was whether the model, that *nota bene* does not include an unknown factor capable of reoxidizing cytosolic NADH, is compatible with the results of Eto et al. [75]. The blocking of the shuttles may be simulated by setting $V_{\text{G3DH}} = 0$, and by reducing V_{AATc} and V_{AATm} . Our strategy for dealing with the overwhelming dimensionality of the parameter space of the model was first, to focus on the most uncertain parameter family: the limiting rates V [76], and second, to identify the limiting rates with the largest flux control coefficients and analyze the model in terms of these parameters. The steady-state behavior of the model for almost 3000 combinations of limiting rates were examined. It turned out that the results of Eto et al. [75] were compatible only with a high activity of V_{ACS} (see **paper IV** for details). A reproduction of the results of Eto et al. [75] are shown in figure 5.4. In this scenario, no unknown factor is needed, since ACS is able to compensate for lost AAT activity, which makes it possible for MDHc to keep up its reoxidation of cytosolic NADH. This is clarified in figure 5.5, which shows the magnitude of the different fluxes in the steady state, with and without blocking of the NADH shuttles.

Having established a model that well describes the coupling between the glycolysis and the TCA cycle in terms of experimental data obtained from β -cells, we examined the input-output relationships between the glycolytic input signal and the different putative output signals: the ATP/ADP ratio (assumed to be proportional to the NADH consumption by respiration), the cytosolic NADPH production (assumed to be proportional to the rate of the IDHP and ME reactions) and malonyl-CoA (assumed to be proportional to the rate of the ACS reaction). This was analyzed in terms of the gains of these output signals. The model predicts significant gains in all three cases (see **paper IV**). The gain in NADPH production is especially strong. Moreover, the gains are attenuated by an increased fatty acid oxidation rate. This phenomenon has been observed experimentally [77], but it is to this date unclear to what extent acute metabolic effects and genetic regulation are responsible for the effect. Our study predicts a significant acute metabolic contribution in this context. The theoretical basis of this is further analyzed in **paper V** in the context of MCA.

Our model furthermore predicts that the flux distribution is dominated by a cycle consisting of, in turn, PC, AAT, AATc, MDHc, and ME. This is seen in the visualisation of the flux distribution in figure 5.6A. The TCA cycle is thus not the main pathway of the β -cell mitochondrial metabolism. If V_{ME} is sufficiently large, the MDH reaction may even proceed in the backward direction (figure 5.6B). This has implications for the interpretation of NMR spectra from ^{13}C -labeled intermediates of the mitochondrial metabolism, a technique that has been used frequently during the last few years to investigate the putative output signals of the K_{ATP} -independent pathway, notably in the studies on the β -cell biochemistry by Schuit et al. [55] and Lu et al. [78].

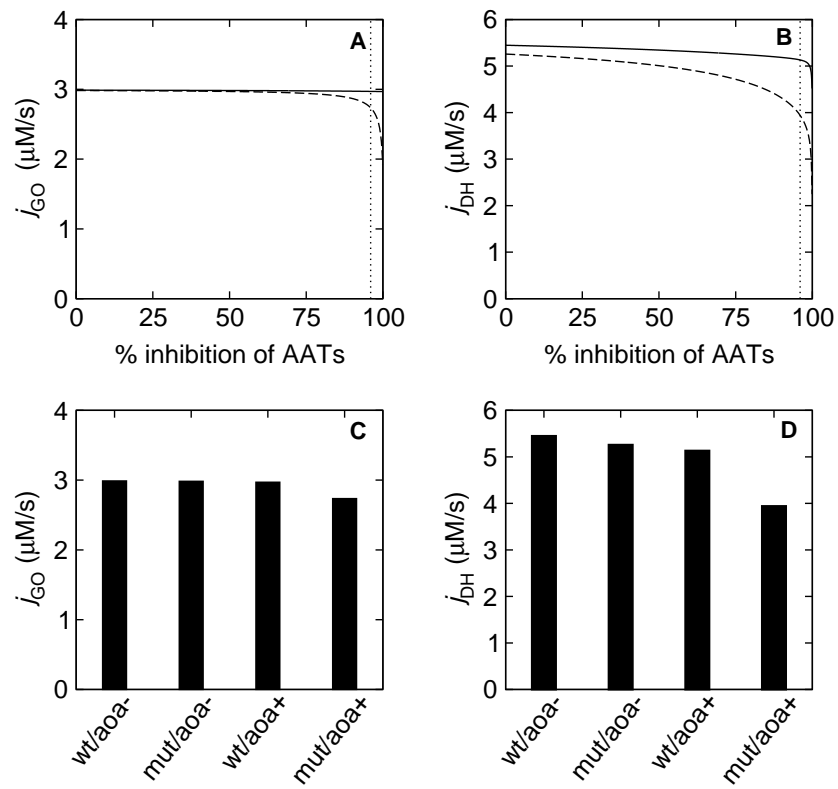


Figure 5.4: **Simulation of the experiments of Eto et al. [75].** Panels A and B: as the inhibition of the AAT enzymes is increased, j_{DH} falls only when there is no G3DH activity. The glycolytic rate j_{GO} is less affected. Panels C and D shows snapshots of panels A and B, taken at 0% inhibition and at 96% inhibition (dotted line). Panels C and D may be directly compared to figure 2 in the paper of Eto et al. [75].

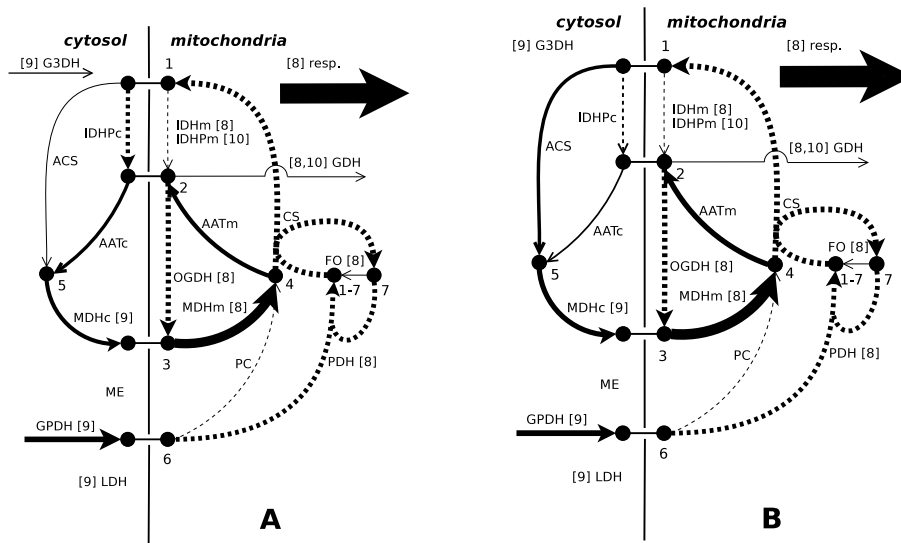


Figure 5.5: **Distribution of fluxes in the simulations of the experiments of Eto et al. [75].** Panel A shows the case with 0% inhibition of the AATs and with no G3DH activity. Panel B shows the case with 96% inhibition of the AATs and also with no G3DH activity. The fluxes are proportional to the line thickness; as a reference, the GPDH flux is 0.3 mM.

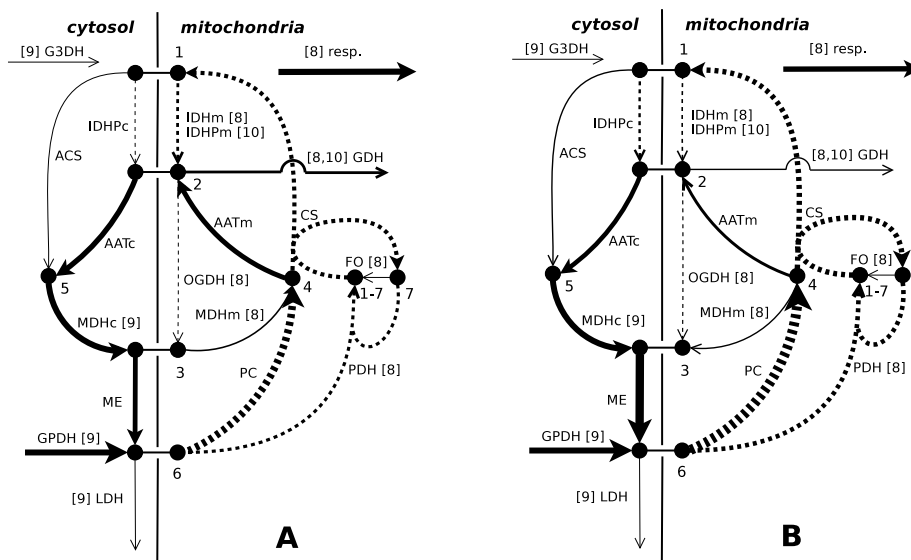


Figure 5.6: **In the general (non-mouse) case, there is ME activity, and the MDH reaction may go backwards.** In both panels, $V_{\text{GPDH}} = 0.015$ and in panel A, $V_{\text{GDH}} = 0.5$ while in panel B, $V_{\text{GDH}} = 0.1$. The thickness of the arrows correspond to the magnitude of the fluxes; as a reference, j_{GPDH} is about $0.3 \mu\text{M}$ in the diagrams.

Modular MCA of the NADH Shuttle System

In the work presented in **paper IV**, a model describing, among other things, the coupling between the glycolysis and mitochondrial metabolism was analyzed numerically in the steady-state and the results of Eto et al. [75] were reproduced. As a complement to this study, I will here make an attempt at an analytical approach to the description of the NADH shuttles, with the help of MCA (described in section 4.2). MCA allows one to express global flux control coefficients in terms of local elasticities, which is a remarkable strength. In practice, however, this is not feasible for a model of our size, since it would require the inversion of a 19×19 matrix of elasticities. This does not mean that theoretical insights into the control of fluxes and steady state concentrations of species are impossible to gain. Consider the scheme in figure 5.7. This is the model described in the previous section and in **paper IV**, with the mitochondria and part of the cytosolic system replaced by a black box, which may be viewed as a “super enzyme”. We will here skip our ambition for a theoretical understanding of the super enzyme, but instead venture to examine the rest of the system as outlined in the figure analytically. We will use the methodology outlined by Schuster et al. [79] and in line with these authors name the super enzyme module 1, and the rest of the system, which is to be investigated analytically, module 2.

We denote NADHc as x_1 and NADc as x_2 . The system depicted in figure 5.7 attains steady-state according to the equation $\mathbf{N}\mathbf{j} = \dot{\mathbf{x}} = 0$, where $\mathbf{j} = (j_{\text{MDH}}, j_{\text{GPDH}}, j_{\text{G3DH}})^T$ and the stoichiometry is described by:

$$\mathbf{N} = \begin{pmatrix} -1 & 1 & -1 \\ 1 & -1 & 1 \end{pmatrix}.$$

The stoichiometry matrix is reduced to the full-rank matrix \mathbf{N}_R via a link matrix \mathbf{L} :

$$\mathbf{N}_R = \begin{pmatrix} -1 & 1 & -1 \end{pmatrix} \quad \text{and} \quad \mathbf{L} = \begin{pmatrix} 1 \\ -1 \end{pmatrix}.$$

We further write the matrix of unscaled elasticities D as

$$\mathbf{D} = \begin{pmatrix} D_1^{\text{MDHc}*} & D_2^{\text{MDHc}*} \\ D_1^{\text{GPDH}*} & D_2^{\text{GPDH}*} \\ D_1^{\text{G3DH}} & D_2^{\text{G3DH}} \end{pmatrix}.$$

Here, the asterisks indicate overall elasticities, where it is assumed that module 1 is allowed to attain steady state and the concentrations of module 2 metabolites are considered to be clamped.

We consider unscaled elasticities, defined $D_2^v = \frac{\partial v}{\partial s_2}$, and we define $D_{12}^v = \frac{\partial v}{\partial x_1} - \frac{\partial v}{\partial x_2}$. We may draw a couple of conclusions already from these simple expressions by using equation 4.2. First, we note that

$$C_{\text{G3DH}}^{\text{MDHc}} = -D_{12}^{\text{MDHc}*} / K, \quad (5.3)$$

where K is defined $K = D_{12}^{\text{G3DH}} + D_{12}^{\text{MDHc}*} - D_{12}^{\text{GPDH}*} > 0$. If $D_{12}^{\text{MDHc}*}$ is positive (i.e. the rate of the MDHc reaction as defined in figure 5.7 increases with increased cytosolic NADH levels), equation 5.3 contains one of the intuitive

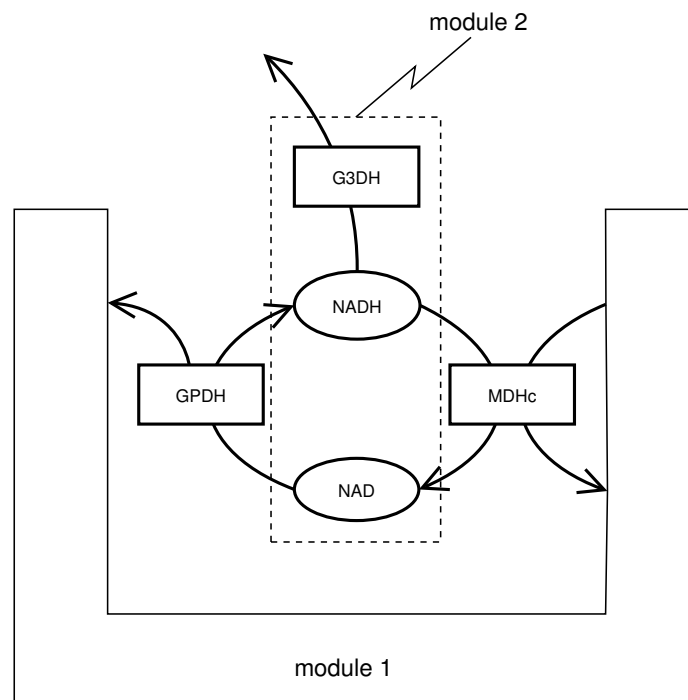


Figure 5.7: **Scheme for modular MCA of the shuttle model.** Metabolites considered explicitly are cytosolic NADH and NAD (module 2), while the rest of the system is a “black box” (module 1). GPDH and MDHc represent bridge reactions. I here omit the LDH reaction which in the numerical investigations (cf. figures 5.5, 5.6 and **paper IV**) exhibits a low flux.

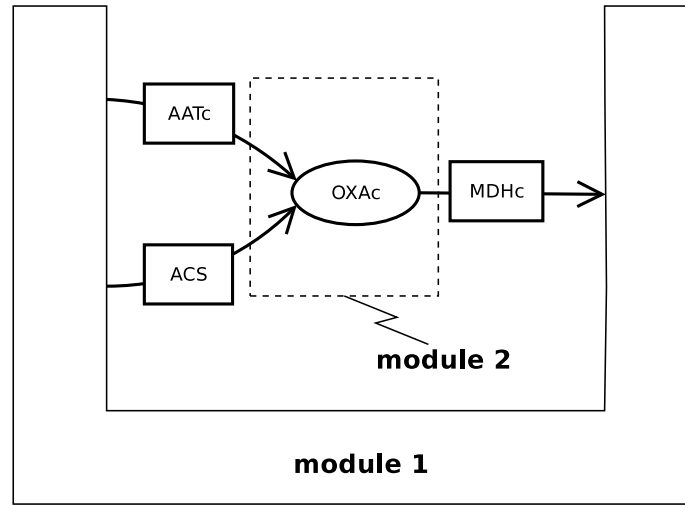


Figure 5.8: **Scheme for modular MCA of the enzymes ACS, AATc and MDHc in the model presented in paper IV.** Here, only cytosolic oxaloacetate is studied explicitly (module 2), while the rest of the model is considered as a “black box” (module 1). Oxaloacetate is abbreviated “oxa”.

reciprocal relationship between the shuttles, we will call it the *first shuttle relationship*. If the activity of G3DH is increased, the flux through the MDHc reaction is decreased. Conversely, we have that

$$C_{\text{MDHc}}^{\text{G3DH}} = -D_{12}^{\text{G3DH}}/K, \quad (5.4)$$

which expresses the *second shuttle relationship*; if the rate of the MDHc reaction is increased, the flux through the G3DH reaction is decreased.

Next, we consider the influences of the activity of the shuttles on the flux through the GPDH reaction. We have that $C_{\text{G3DH}}^{\text{GPDH}} = C_{\text{MDHc}}^{\text{GPDH}} = -D_{12}^{\text{GPDH}^*}/K$. This quantity is, judged from intracellular NAD(H)c levels together with estimations of the binding constants (presented in **paper IV**), quite low. Thus, the NADHc/NADc ratio would have to be raised immensely before, e.g., an abolishment of the shuttles would influence the glycolytic flux via catastrophic inhibition of GPDH. It is plausible that a close to normal NADHc/NADc ratio may be maintained in spite of G3DH and AATc being inactivated, by means of flux through the ACS and MDHc reactions. I argue that this is an attractive alternative to the assumption of an unknown NADHc consumer [80].

In order to relate how an abolishment of the AATc reaction affects the MDHc and ACS reactions, I performed the same type of analysis of the reaction scheme defined by figure 5.8. All elasticities in this analysis are overall elasticities, which have to be evaluated letting all variables in module 1 attain steady state. Let us make the following assumptions: $D_1^{\text{MDH}} > 0$, $D_1^{\text{ACS}} < 0$ and $D_1^{\text{AATc}} < 0$, where 1 refers to oxaloacetate. Then we may draw some conclusions: first, we have

$$C_{\text{AATc}}^1 = 1/K > 0,$$

where $K = D_1^{\text{MDH}} - D_1^{\text{ACS}} - D_1^{\text{AATc}} > 0$. Thus, the cytosolic oxaloacetate levels

will always follow that of the AATc activity. Second, we have

$$C_{\text{AATc}}^{\text{ACS}} = D_1^{\text{ACS}}/K < 0.$$

This expression tells us to which extent ACS compensates for lost AATc activity. We may note here that AATc, ACS, and MDHc operate at different points if G3DH is active or not — G3DH affects MDHc according to the first shuttle relationship (equation 5.3). This may explain the differences in TCA cycle activities observed by Eto et al. [75], when G3DH is present or not, since ACS and AATc are linked to the TCA cycle via the metabolites citrate and 2-oxoglutarate.

Third, we have

$$C_{\text{AATc}}^{\text{MDHc}} = D_1^{\text{MDHc}}/K > 0.$$

If D_1^{MDHc} is normally very close to zero — i.e. the MDHc reaction is saturated with respect to oxaloacetate — the second and third conclusions together quantitatively express our hypothesis that during normal conditions, ACS is able to compensate for lost AATc activity. This allows MDHc to continue to reoxidize NADH; a modulation of AATc activity reciprocally affects the ACS flux but leaves the MDHc flux virtually unchanged. However, ultimately, as V_{AATc} is decreased, the cytosolic oxaloacetate level, which follow the activity of AATc as stated above, might sink to sufficiently low levels that D_1^{MDHc} will become significant. Then it would be reasonable to assume that, according to the second shuttle relationship (equation 5.4), the G3DH reaction will increase its rate to compensate. This is impossible in the case G3DH is abolished. In this case, the NADHc/NADc ratio would start to rise dramatically, and the shuttle system would break down, resulting in a halted glycolysis. However, this does not seem to be the case in the experiments of Eto et al. [75], which suggests that the cytosolic oxaloacetate concentration never reaches these low levels, and that ACS is able to compensate and maintain a sufficiently high cytosolic oxaloacetate level so that $C_{\text{AATc}}^{\text{MDHc}}$ stays low even at very low AATc rates.

Fourth, and finally, we note that

$$C_{\text{MDH}}^{\text{AATc}} = -D_1^{\text{AAT}}/K > 0,$$

and that

$$C_{\text{MDH}}^{\text{ACS}} = -D_1^{\text{ACS}}/K > 0.$$

Let us recall that a modulation of the G3DH rate mainly affects the MDHc rate (since the NADc/NADHc influence on the GPDH rate is small). Then, we have arrived at an approximate quantitative description of the experimentally noted compensatory effects between the NADH shuttles; if the G3DH reaction is abolished, resulting in an increase of the rate of the MDHc reaction mediated by the NADc/NADHc levels, the ACS and AATc together compensate for the increased flux through the malate-aspartate shuttle.

MCA of the Anaplerosis

The results presented in **paper IV** indicated that the fatty acid oxidation (FO) via the metabolism, i.e. without any genetic regulation, may affect GSIS by increasing the mitochondrial metabolism, while blunting the response to a raised glycolytic flux. This has indeed been seen experimentally. It constitutes a part

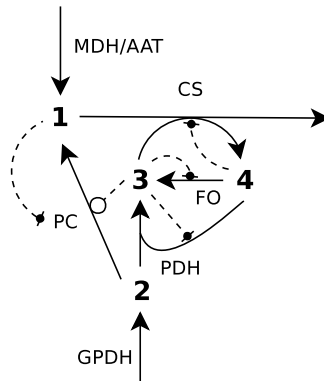


Figure 5.9: **The carbon influx to the mitochondrial metabolism.** The numbers refer to four variables which represent different metabolites; x_1 = oxaloacetate, x_2 = pyruvate, x_3 = ac-CoA, x_4 = CoA. The solid arrows represent mass flux. The dashed arrows represent modulation of enzyme activity by the metabolites; the open circle represents ac-CoA activation of PC, while the filled circles/bars represent product inhibition of PC, CS, FO, and PDH. The MDH flux is here the lumped together with the AAT flux without loss of generality.

of the development of insulin deficiency called *lipotoxicity* [81]. In this context, the so-called Randle cycle, which defines an inhibitory influence by FO on glucose oxidation, is thought to be operative, via fatty acid inhibition of PDH and citrate inhibition of PFK [82]. Especially PDH is thought to be crucial in this respect, since it is heavily regulated both via metabolite modulation and by phosphorylation and dephosphorylation.

In the study presented in **paper V**, the objective was to gain a better theoretical understanding of the interface between the glycolysis, FO, and the mitochondrial metabolism. Also, we investigated how FO may influence the anaplerotic flux, something that to our knowledge still has to be done experimentally. Further, we investigated the effect of PDH regulation on FO and anaplerosis. For this, we considered the enzymatic reactions depicted in figure 5.9, which constitute a part of the larger system of **paper IV**. Here, however, we employed the methods of MCA for the analysis. This enables the exact expression of different control coefficients in terms of elasticities. The analytical results thus obtained are more general than the numerical results of **paper IV**, since they are not hampered by the inexhaustive inventory of a huge parameter space. The drawback is that they are limited to a smaller part of the metabolism.

The steady-states of this system are solutions to the equation $\mathbf{N}\mathbf{j} = \dot{\mathbf{x}} = 0$, where $\mathbf{x} = (x_1, x_2, x_3, x_4)^T$, and $\mathbf{j} = (j_{\text{PDH}}, j_{\text{PC}}, j_{\text{CS}}, j_{\text{M/A}}, j_{\text{GPDH}}, j_{\text{FO}})^T$, where M/A denotes MDH/AAT. The stoichiometry is described by

$$\mathbf{N} = \begin{pmatrix} 0 & 1 & -1 & 1 & 0 & 0 \\ -1 & -1 & 0 & 0 & 1 & 0 \\ 1 & 0 & -1 & 0 & 0 & 1 \\ -1 & 0 & 1 & 0 & 0 & -1 \end{pmatrix}.$$

The matrix \mathbf{N} is reduced to the full-rank matrix \mathbf{N}_R , via a the link matrix \mathbf{L} so that $\mathbf{N} = \mathbf{L}\mathbf{N}_R$, accordingly:

$$\mathbf{N}_R = \begin{pmatrix} 0 & 1 & -1 & 1 & 0 & 0 \\ -1 & -1 & 0 & 0 & 1 & 0 \\ 1 & 0 & -1 & 0 & 0 & 1 \end{pmatrix} \quad \text{and} \quad \mathbf{L} = \begin{pmatrix} 1 & 0 & 0 \\ 0 & 1 & 0 \\ 0 & 0 & 1 \\ 0 & 0 & -1 \end{pmatrix}.$$

We write the matrix \mathbf{D} of unscaled elasticities as (see figure 5.9):

$$\mathbf{D} = \begin{pmatrix} 0 & D_2^{\text{PDH}} & D_3^{\text{PDH}} & D_4^{\text{PDH}} \\ D_1^{\text{PC}} & D_2^{\text{PC}} & D_3^{\text{PC}} & 0 \\ D_1^{\text{CS}} & 0 & D_3^{\text{CS}} & D_4^{\text{CS}} \\ D_1^{\text{M/A}} & 0 & 0 & 0 \\ 0 & 0 & 0 & 0 \\ 0 & 0 & D_3^{\text{FO}} & D_4^{\text{FO}} \end{pmatrix}.$$

We may make the signs of the elasticities explicit, according to the mass flow and modulatory interactions defined in figure 5.9:

$$\text{sgn}(\mathbf{D}) = \begin{pmatrix} 0 & 1 & -1 & 1 \\ -1 & 1 & 1 & 0 \\ 1 & 0 & 1 & -1 \\ -1 & 0 & 0 & 0 \\ 0 & 0 & 0 & 0 \\ 0 & 0 & -1 & 1 \end{pmatrix}.$$

Here it is assumed that $D_1^{\text{M/A}} < 0$. Strictly, $D_1^{\text{M/A}}$ should be viewed as an overall elasticity which should be measured by varying x_1 while keeping x_2 , x_3 and x_4 constant. It is not entirely trivial to determine the sign of $D_1^{\text{M/A}}$; cf. **paper V**. Note also that we have neglected any feedback on the rate of the glucose oxidation rate.

I will here account for a representative selection of the results presented in **paper V**. Proceeding with the differentiation according to equation 4.2 and taking $\text{sgn}(\mathbf{D})$ into consideration, we find that

$$C_{\text{FO}}^{\text{PDH}} = (-D_1^{\text{CS}}D_2^{\text{PDH}}D_3^{\text{PC}} + D_1^{\text{PC}}D_2^{\text{PDH}}D_3^{\text{CS}} + D_1^{\text{M/A}}D_2^{\text{PC}}D_3^{\text{PDH}} + D_1^{\text{M/A}}D_2^{\text{PDH}}D_3^{\text{PC}} - D_1^{\text{CS}}D_2^{\text{PC}}D_3^{\text{PDH}})/K < 0, \quad (5.5)$$

where

$$K = -D_1^{\text{M/A}}D_2^{\text{PDH}}D_3^{\text{PC}} - D_1^{\text{M/A}}D_2^{\text{PC}}D_3^{\text{FO}} - D_1^{\text{M/A}}D_2^{\text{PDH}}D_3^{\text{CS}} - D_1^{\text{PC}}D_2^{\text{PDH}}D_3^{\text{FO}} + D_1^{\text{CS}}D_2^{\text{PDH}}D_3^{\text{FO}} + 2D_1^{\text{CS}}D_2^{\text{PC}}D_3^{\text{PDH}} - 2D_1^{\text{PC}}D_2^{\text{PDH}}D_3^{\text{CS}} - D_1^{\text{M/A}}D_2^{\text{PDH}}D_3^{\text{FO}} + D_1^{\text{CS}}D_2^{\text{PC}}D_3^{\text{FO}} - D_1^{\text{M/A}}D_2^{\text{PC}}D_3^{\text{PDH}} - D_1^{\text{M/A}}D_2^{\text{PC}}D_3^{\text{CS}} + 2D_1^{\text{CS}}D_2^{\text{PDH}}D_3^{\text{PC}} > 0.$$

Further,

$$C_{\text{FO}}^{\text{PC}} = -C_{\text{FO}}^{\text{PDH}} > 0, \quad (5.6)$$

and

$$C_{\text{FO}}^{\text{CS}} = (D_1^{\text{CS}} D_2^{\text{PDH}} D_3^{\text{PC}} + D_1^{\text{CS}} D_2^{\text{PC}} D_{34}^{\text{PDH}} - D_1^{\text{M/A}} D_2^{\text{PDH}} D_{34}^{\text{CS}} - D_1^{\text{M/A}} D_2^{\text{PC}} D_{34}^{\text{CS}} - D_1^{\text{PC}} D_2^{\text{PDH}} D_{34}^{\text{CS}}) / K > 0. \quad (5.7)$$

Equation 5.5 ascertains that an increased FO flux will decrease the flux via PDH by means of acute metabolic regulation. The expression contains five terms, all negative, only two of which contain the factor representing ac-CoA inhibition of PDH: D_{34}^{PDH} . This is the feedback interaction usually thought to constitute a metabolic cause of the Randle effect of FO on PDH. Two of the remaining terms contain the factor D_3^{PC} and thus represent regulation via (dependent on) ac-CoA activation of PC. There is also the term containing the factors $D_1^{\text{PC}} D_{34}^{\text{CS}}$, which represent regulation of PC by oxaloacetate and regulation of CS by CoA and ac-CoA. These three latter terms contribute to FO down-regulation of PDH activity, although this is not intuitively clear from a quick inspection of the visual representation of the system (figure 5.9). Hence, these interactions have (to our knowledge) never been pointed out when discussing FO regulation of the PDH flux. Furthermore, phosphorylation of PDH, which is activated by ac-CoA, will further down-regulate the PDH activity on a longer timescale. Equation 5.6 asserts that the PC flux is increased by FO, while the PDH flux is decreased. Thus, the anaplerotic flux is increased by FO. This is also qualitatively in agreement with the numerical results presented in **paper IV**, which pertain to the larger model depicted in figure 5.3. This prediction has important implications for the β -cell. Since the anaplerotic flux is positively correlated to insulin secretion via the K_{ATP} -independent pathway, an increased FO should potentiate this pathway. Also, equation 5.7 tells us that an increased FO increases the total flux via CS regardless of whether CS is sensitive to CoA and ac-CoA.

We furthermore find that

$$C_{\text{PDH}}^{\text{PC}} = D_2^{\text{PC}} (D_1^{\text{M/A}} D_{34}^{\text{CS}} - D_1^{\text{CS}} D_{34}^{\text{FO}} + D_1^{\text{M/A}} D_{34}^{\text{FO}}) / K < 0, \quad (5.8)$$

and that

$$C_{\text{PDH}}^{\text{FO}} = D_2^{\text{PC}} D_{34}^{\text{FO}} (D_1^{\text{M/A}} - 2D_1^{\text{CS}}) / K < 0.$$

Thus, an increased PDH activity will lower the anaplerotic flux *and* the FO. The latter is precisely along the conventional thinking of this part of the mitochondrial metabolism. PDH is thought to be down-regulated via phosphorylation during starvation, in order to stimulate FO and lower the glucose usage. The reciprocal relationship between PDH and PC flux expressed by equation 5.8 suggests that the anaplerosis is attenuated by an activation of PDH. Whether this property of the part of the mitochondrial metabolism analyzed here is valid in the intact β -cell should be analyzed experimentally.

Several more derivations like the ones described above were made in **paper V**. I here summarize the main conclusions from the study:

- PDH exerts negative control over FO, but not on GO.
- PDH exerts negative control over the anaplerosis.
- FO exerts control over PDH via several interactions in addition to the regulation by CoA and ac-CoA.

- Increased FO will increase anaplerosis, but not necessarily so-called pyruvate cycling.
- Increased Ca^{2+} concentration does not stimulate anaplerosis.
- PDH exerts positive control over the M/A reaction, while PC exerts negative control over it.
- CS and FO are interregulated via a negative feedback loop.
- The intracellular milieu in the β -cell is optimized for control by PDH.
- Ultrasensitivity in the regulation by GO over the anaplerosis is possible.

On Oscillations in the TCA Cycle

Recently, MacDonald et al. [83] made the remarkable observation of sustained minute-scale oscillations in citrate levels in isolated mitochondria from liver, pancreatic islets, and INS-1 insulinoma cells and in intact INS-1 cells. The biochemical mechanism behind these oscillation is unknown, but since they occurred in isolated mitochondria, a glycolytic origin is ruled out. The authors proposed a putative mechanism for the generation of these oscillations, and I cite from their paper:

“A plausible explanation for the regulation of citrate oscillations can be formulated on the basis of our current data plus what is known from decades of research on the citric acid cycle. Within an individual oscillation, as the citrate level increases and then plateaus, its rate of synthesis should begin to decrease because citrate synthase is inhibited by its product citrate and also by succinyl-CoA, the product of the α -ketoglutarate dehydrogenase reaction. In addition, the citrate level should decrease via its metabolism. A high NAD level should favor increased flux through the reactions catalyzed by NAD-isocitrate dehydrogenase and α -ketoglutarate dehydrogenase, thus increasing the rate of citrate metabolism. The fact that the citrate profile exactly mirrors the NAD(P) profile in INS-1 cell mitochondria is consistent with this idea. Concomitantly with the metabolism of citrate, the NAD level will decrease from its reduction to NADH, and the NADH level will increase. The resulting lower NAD/NADH ratio will decrease flux through the dehydrogenase reactions. As the citrate and the NAD/NADH ratio reach their nadirs, the low citrate level will permit its rate of synthesis to increase, and the low NAD/NADH ratio will slow the rate of citrate metabolism. This will contribute to the ascending part of the citrate profile.”

This is a striking example of how the verbal expression of a dynamical model may be insufficient for the assessment of its behavior, as mentioned in the introduction of this thesis. Let us reformulate the model described above as a two-dimensional dynamical system, as schematically depicted in figure 5.10. This model is a condensed version of the verbal model cited above. The only thing not included is the inhibition by succinyl-CoA of CS, which we will return to later. The reaction “ox” is the NAD consumption by other dehydrogenases than IDH, and NADH consumption lumped together, i.e.

$$v_{\text{ox}} = v_{\text{NADH cons.}} - v_{\text{NAD cons.}}$$

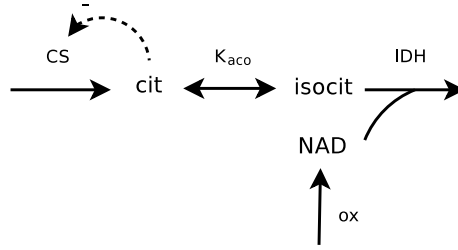


Figure 5.10: **Scheme of the metabolites and reactions proposed by MacDonald et al. [83]** to generate oscillations in the mitochondrial metabolism. IDH stands for isocitrate dehydrogenase, while K_{aco} is the equilibrium constant of the aconitase catalyzed reaction.

Denoting the citrate concentration as σ and the NAD concentration as ν , the model may be formulated as an ODE system:

$$\begin{aligned}\dot{\sigma} &= f \times (v_{cs}(\sigma) - f \times v_{IDH}(\sigma, \nu)) \\ \dot{\nu} &= v_{ox}(\nu) - v_{IDH}(\sigma, \nu).\end{aligned}\quad (5.9)$$

where, just as in the model described in **paper IV**, the aconitase reaction, which converts citrate to isocitrate, is considered to be in quasi-equilibrium with equilibrium constant K_{aco} , which yields the factor $f = 1/(1 + K_{aco})$. We use the theory described in section 4.4 and examine the trace of the Jacobian \mathcal{J} of the system:

$$\text{Tr}\mathcal{J} = f \times \left(\frac{\partial v_{CS}}{\partial \sigma} - \frac{\partial v_{IDH}}{\partial \sigma} \right) + \frac{\partial v_{ox}}{\partial \nu} - \frac{\partial v_{IDH}}{\partial \nu} < 0.$$

The trace has to be negative, since all its terms are negative. This is fairly easy to see. In the case of $\frac{\partial v_{ox}}{\partial \nu}$, we note that $v_{NADH\text{ cons.}}$ has to decrease with an increasing NAD concentration, if the pool $NAD + NADH$ is assumed to be constant and the NADH consumption is assumed to be positively influenced by NADH and possibly negatively influenced by NAD. Also, $v_{NAD\text{ cons.}}$ should increase with increasing NAD concentration if product inhibition by NADH of the dehydrogenase reactions has not taken over completely. We also examine the determinant Δ of the Jacobian:

$$\Delta = f \times \left(\frac{\partial v_{ox}}{\partial \nu} \left(\frac{\partial v_{CS}}{\partial \sigma} - \frac{\partial v_{IDH}}{\partial \sigma} \right) - \frac{\partial v_{CS}}{\partial \sigma} \frac{\partial v_{IDH}}{\partial \nu} \right) > 0.$$

From table 4.1 it immediately becomes clear that a fixpoint of system 5.9 is stable; either a node or a spiral node. The description of MacDonald et al. [83] cited above concerns only the case when the fixpoint is a spiral node. The verbal description is correct in its logic but not sufficient to explain the whole picture. It misses the fact that the fixpoint is an attractor. The oscillations it describes will eventually vanish, and thus, if we forget the inhibition by succinyl-CoA of CS which was mentioned only in passing in the verbal description, the proposed model of MacDonald et al. [83] is *not* a plausible candidate for generating sustained oscillations in the citrate concentration. Now, if we consider also the inhibition by succinyl-CoA of CS, the picture actually becomes slightly

different. A negative feedback *with delay*, i.e. from a metabolite several enzymatic steps away from the inhibited enzyme, may form the core of an oscillator [84]. This grants the possibility that the inhibition of CS by succinyl-CoA *may* cause the system to oscillate. An investigation of the plausibility of this given the peculiarities of the TCA cycle is certainly warranted.

Chapter 6

Conclusions: Summary of Results and Suggestions for Further Investigations

The β -cell is beginning to emerge as a classic in the field of biophysical modeling. The field of theoretical β -cell research dates back to when the complex dynamical patterns of its electrophysiology was examined in a mathematical model by Chay and Keizer [85]. This classic paper is a showcase of how the interplay between quantitative theory and experimental research is vital to scientific progress. The model predicted sawtooth-shaped fast Ca^{2+} oscillations. The shape of the oscillations were subsequently shown to resemble square-waves, which led to refinements of the theoretical model and a better understanding of the mechanisms behind the fast electrical activity (see **paper III** for a review of the early β -cell models). Since the appearance of this paper, there has been a continuous stream of modeling studies concerning the β -cell electrophysiology [86], see also **paper III**.

This thesis addresses a research area previously poorly covered by theoretical modeling: the metabolism of the β -cell. The models developed here cover the glycolysis and the mitochondrial metabolism and address crucial hypotheses concerning GSIS such as oscillations in the glycolysis and cataplerotic fluxes. Below, I suggest how the models could be developed further, and how they could be connected to other models of the β -cell. In fact, the GSIS of the β -cell presents a peculiar challenge for the scientific community in the sense that it involves both metabolic and electrical events. To my knowledge, few biophysical modeling studies have integrated these two areas. The study of Bertram et al. [87] is one of those few. This study integrates an earlier glycolysis model [88] with an unvalidated phenomenological model for the coupling between the glycolysis and mitochondrial ATP production [89], where $d\text{ATP}/dt \propto \text{ATP} - \text{ADP} \times e^{(1+v_{\text{GPDH}})f(\text{Ca}^{2+})/\tau}$, with $f(\text{Ca}^{2+})$ being negatively proportional to the Ca^{2+} concentration and τ being a time constant. It is hoped that the models presented in this thesis fills some of the gaps in those models. I here take the opportunity to summarize the main conclusions of the present thesis.

- The theoretical model of β -cell glycolysis (**paper I**) supports the notion that the glycolysis is inherently oscillatory at sufficiently high glucose influx. The enzyme aldolase is proposed to be important for the glucose influx threshold between the stationary and oscillatory states. The enzyme phosphofructokinase is proposed to control the oscillation frequency.
- The generalized reversible Hill equation derived in **paper II** is shown to describe the complex kinetics of mammalian muscle type phosphofructokinase (the type found in the β -cell) better than, to my knowledge, any previously proposed equation. Yet, the generalized reversible Hill equation has fewer and operationally more well-defined parameters than any previous equation concerning this enzyme.
- A model of the mitochondrial metabolism of the β -cell was presented in **paper IV**. The model, sporting ten dynamic variables, describes the TCA cycle, glycolytic pyruvate production, and the NADH shuttles. The model successfully reproduces much empirical data. It predicts a particularly strong glucose induced signal to cytosolic NADPH production, which encourages further experimental investigation of this putative coupling factor of GSIS (see figure 1.2). The model further predicts that the mitochondrial malate dehydrogenase reaction may be pulled in the backwards direction by the malic enzyme reaction.
- A metabolic control analysis of the interface between the glycolysis and the mitochondrial metabolism (**paper V**) reveals that fatty acid oxidation always will stimulate the anaplerosis. Pyruvate dehydrogenase, a heavily regulated enzyme, exerts negative control over the fatty acid oxidation rate and the anaplerosis, and the biochemical milieu of the β -cell seems to be optimized for PDH to exert its control.
- The biochemical design of the β -cell allows for ultrasensitivity of the anaplerosis to the GO rate (**paper V**).
- The numerical results of **paper IV** concerning the NADH shuttles and the experimental results of Eto et al. [75] have been given a theoretical explanation based on modular metabolic control analysis (section 5.2).
- The notion that citrate inhibition of citrate synthase is the basis of the oscillations in mitochondrial metabolism found recently [83] is proposed to be flawed (section 5.2).

A consistent ambition of the work that constitute this thesis has been to, based on the modeling work, generate experimentally testable predictions (falsifiable in the language of Popper). This has been done in the hope that the theories may give ideas to experimental work whose outcome leads to the refinement (or revolutionary refutation) of the theoretical model: in other words to spawn the fruitful interplay between theory and experiments, which has such a venerable history in other natural sciences such as chemistry, physics and meteorology.

I finally want to remark on a more general methodological topic. In this thesis, I have presented analyses not of the biochemistry of the entire β -cell, but of different *modules* thereof: the glycolysis, NADH shuttles/TCA cycle, the entry point of carbons into the TCA cycle, and of citrate/isocitrate formation

and degradation. This was certainly done in the belief that an understanding of these modules is valuable also in the context of understanding an entire β -cell. This belief was elegantly rationalized by Simon [90] who envisioned the interactions of the cellular metabolism as described by an interaction matrix, which supposedly could be put in something close to block-diagonal form. The author argues that the entire metabolism may be possible to understand via the more fundamental understanding of the modules that constitute it. A more recent discussion on this matter [91] reaches basically the same conclusions.

6.1 Proposals for Further Research

During the course of the studies presented in this thesis, several ideas have come to my mind that I have not had time to pursue. I briefly list some of these below. The list is focused on the synthesis of the existing models to new models with a somewhat broader scope, i.e. to connect parts or modules aiming for a better understanding of “the whole”. I want to emphasize that this probably is not the same as literally connecting the models in the sense that all variables and parameters are retained. Rather, intelligent simplifications need to be made. The level of description suitable when analysing the behaviour of a module is probably not the same level suitable for analysis of the whole. The list below will take hard work and a long time to complete for the serious scientists who aim for scientific quality and clarity. But last but not least it also has the potential to be a genuinely fun and stimulating work.

- A model of the ATP production and the control thereof by the mitochondrial metabolism and Ca^{2+} needs to be developed — perhaps using the model of Magnus and Keizer [92] as a template. This model could be connected to the TCA cycle model presented in chapter 5.2 and **paper IV** to form a more complete picture of the mitochondrial metabolism. In particular, the controversial question whether Ca^{2+} activates or inhibits ATP production (see figure 6.1) should be addressed. Another path of investigation may be to analyze how Ca^{2+} feedback on the regulation of PDH affects the anaplerosis (c.f. the discussion in section 5.2). The search for a possible mechanism responsible for the generation of citrate oscillations in isolated mitochondria could also be pursued with the aid of such a model.
- The model of mitochondrial metabolism could be connected with the existing glycolysis model. A central question is then how feedback by ATP, AMP and citrate influence the control of slow glycolytic oscillations.
- The unified model of the glycolysis and mitochondria may then be connected with existing models of β -cell electrophysiology. Important connection points will be the intracellular calcium concentration (which affects the metabolism e.g. via the mitochondria) and the ATP/ADP ratio. Also, a possible feedback of calcium on the glycolytic oscillation generator, PFK, may be operative via calmodulin [94].
- Probably only about 50 insulin granules are organized in a “readily releasable pool” [95], whilst recruiting of “dormant” granules is necessary

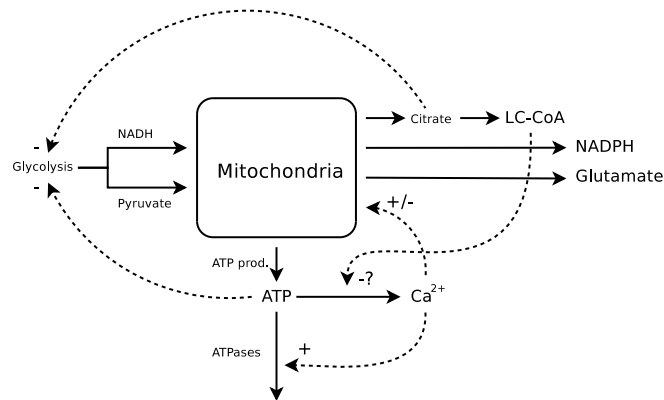


Figure 6.1: The scheme in figure 1.2 is here elaborated. The influence of Ca^{2+} on the ATP homeostasis is complex, with Ca^{2+} either inhibiting or activating mitochondrial ATP production and activating ATP consumption by ATPases. Citrate and ATP inhibit PFK [39], and LC-CoA may affect the K_{ATP} -channel [93].

for normal insulin secretion. How should this insulin release system be modeled? Insulin release was modeled as long as thirty years ago by Grodsky [96, 97]. It is time for the theories developed in these studies to be updated.

- The glycolysis model of **paper I** is certainly amenable for further development. For instance, how might PFK-2 [98], which converts FBP to fructose-2,6-bisphosphate, an activator of PFK, affect the behavior of the β -cell glycolysis?
- The FO and, specifically, the feedback loop via malonyl-CoA and CPT-1 is a suitable subject for further modeling studies.
- The creatine/phosphocreatine system can be viewed as spatial and temporal buffers both in the cytosol as well as in the mitochondria and is operative in the β -cell [99]. Its role in regulating β -cell ATP/ADP ratio and activation of the K^+ -ATP channels should be investigated theoretically.
- The critical reader has noted that the models in this thesis pertain to single β -cells. While individual β -cells exhibit a great deal of variability in the frequency of e.g. Ca^{2+} oscillations, β -cells within an islet are synchronized, and the frequency of whole islet oscillations vary to a lesser degree. Since the cells within an islet are electrically and chemically coupled, a fuller understanding of the behavior of islets demands modeling studies executed on a multicellular level. Early studies on this subject [100] were fruitful, and it should soon be time to integrate the metabolism into this kind of models. Recent experimental data points towards ATP being an important player in the synchronization of β -cell oscillations [101] which should be taken into consideration in the modeling work. Yet another question is how different islets synchronize to generate the insulin pulses

seen on a physiological level. There is here room for the employment of general theories for the synchronization of biological oscillators [102].

Bibliography

- [1] Wold, S., Sjöström, M., Carlson, R., Lundstedt, T., Hellberg, S., Skagerberg, B., Wikström, C., and Öhman, J. (1986). Multivariate Design. *Analytica Chimica Acta*, 191:17–32.
- [2] Färnkvist, L. M. and Lundman, B. M. (2003). Outcomes of diabetes care: a population-based study. *Int J Qual Health Care*, 15:301–7.
- [3] Zimmet, P. (2003). The burden of type 2 diabetes: are we doing enough? *Diabetes Metab*, 29:6S9–18.
- [4] Groop, L. C. (1999). Insulin resistance: the fundamental trigger of type 2 diabetes. *Diabetes Obes Metab*, 1 Suppl 1:S1–7.
- [5] Hedekov, C. J. (1980). Mechanism of glucose-induced insulin secretion. *Physiol Rev*, 60:442–509.
- [6] Straub, S. G. and Sharp, G. W. (2002). Glucose-stimulated signaling pathways in biphasic insulin secretion. *Diabetes Metab Res Rev*, 18:451–63.
- [7] Ashcroft, F. M. and Rorsman, P. (1989). Electrophysiology of the pancreatic beta-cell. *Prog Biophys Mol Biol*, 54:87–143.
- [8] Lang, D. A., Matthews, D. R., Peto, J., and Turner, R. C. (1979). Cyclic oscillations of basal plasma glucose and insulin concentrations in human beings. *N. Engl. J. Med.*, 301:1023–1027.
- [9] Bergsten, P. and Hellman, B. (1993). Glucose-induced amplitude regulation of pulsatile insulin secretion from individual pancreatic islets. *Diabetes*, 42:670–674.
- [10] Jonas, J.-C., Gilon, P., and Henquin, J.-C. (1998). Temporal and quantitative correlations between insulin secretion and stably elevated or oscillatory cytoplasmic Ca^{2+} in mouse pancreatic β -cells. *Diabetes*, 47:1266–1273.
- [11] Porksen, N. (2002). The in vivo regulation of pulsatile insulin secretion. *Diabetologia*, 45:3–20.
- [12] Goldbeter, A. (2002). Computational approaches to cellular rhythms. *Nature*, 420:238–45.

- [13] Li, Y. and Goldbeter, A. (1989). Frequency specificity in intercellular communication. Influence of patterns of periodic signaling on target cell responsiveness. *Biophys J*, 55:125–45.
- [14] Paolisso, G., Scheen, A. J., Giugliano, D., Sgambato, S., Albert, A., Varicchio, M., D'Onofrio, F., and Lefebvre, P. J. (1991). Pulsatile insulin delivery has greater metabolic effects than continuous hormone administration in man: importance of pulse frequency. *J Clin Endocrinol Metab*, 72:607–15.
- [15] Grubert, J. M., Lautz, M., Lacy, D. B., Moore, M. C., Farmer, B., Penaloza, A., Cherrington, A. D., and McGuinness, O. P. (2005). Impact of continuous and pulsatile insulin delivery on net hepatic glucose uptake. *Am J Physiol Endocrinol Metab*, 289:E232–40.
- [16] Tornheim, K. (1997). Are metabolic oscillations responsible for normal oscillatory insulin secretion? *Diabetes*, 46:1375–1380.
- [17] Deeney, J. T., Gromada, J., Hoy, M., Olsen, H. L., Rhodes, C. J., Prentki, M., Berggren, P. O., and Corkey, B. E. (2000). Acute stimulation with long chain acyl-CoA enhances exocytosis in insulin-secreting cells (HIT T-15 and NMRI beta-cells). *J Biol Chem*, 275:9363–8.
- [18] Corkey, B. E., Glennon, M. C., Chen, K. S., Deeney, J. T., Matschinsky, F. M., and Prentki, M. (1989). A role for malonyl-CoA in glucose-stimulated insulin secretion from clonal pancreatic beta-cells. *J Biol Chem*, 264:21608–12.
- [19] Deeney, J. T., Cunningham, B. A., Chheda, S., Bokvist, K., Juntti-Berggren, L., Lam, K., Korchak, H. M., Corkey, B. E., and Berggren, P. O. (1996). Reversible Ca²⁺-dependent translocation of protein kinase C and glucose-induced insulin release. *J Biol Chem*, 271:18154–60.
- [20] Watkins, D. T. and Moore, M. (1977). Uptake of NADPH by islet secretion granule membranes. *Endocrinology*, 100:1461–7.
- [21] MacDonald, M. J. (1995). Feasibility of a mitochondrial pyruvate malate shuttle in pancreatic islets. Further implication of cytosolic NADPH in insulin secretion. *J Biol Chem*, 270:20051–8.
- [22] Laclau, M., Lu, F., and MacDonald, M. J. (2001). Enzymes in pancreatic islets that use NADP(H) as a cofactor including evidence for a plasma membrane aldehyde reductase. *Mol Cell Biochem*, 225:151–60.
- [23] Maechler, P. and Wollheim, C. B. (1999). Mitochondrial glutamate acts as a messenger in glucose-induced insulin exocytosis. *Nature*, 402:685–9.
- [24] Maechler, P. (2002). Mitochondria as the conductor of metabolic signals for insulin exocytosis in pancreatic beta-cells. *Cell Mol Life Sci*, 59:1803–18.
- [25] MacDonald, M. J. and Fahien, L. A. (2000). Glutamate is not a messenger in insulin secretion. *J Biol Chem*, 275:34025–7.

- [26] Mulder, H., Lu, D., Finley, 4th, J., An, J., Cohen, J., Antinozzi, P. A., McGarry, J. D., and Newgard, C. B. (2001). Overexpression of a modified human malonyl-CoA decarboxylase blocks the glucose-induced increase in malonyl-CoA level but has no impact on insulin secretion in INS-1-derived (832/13) beta-cells. *J Biol Chem*, 276:6479–84.
- [27] Nicolis, G. and Prigogine, I. (1977). *Self-organization in nonequilibrium systems*. John Wiley & Sons.
- [28] Alberty, R. A. (1998). Calculation of standard transformed formation properties of biochemical reactants and standard apparent reduction potentials of half reactions. *Arch Biochem Biophys*, 358:25–39.
- [29] Alberty, R. A. (1998). Calculation of standard transformed Gibbs energies and standard transformed enthalpies of biochemical reactants. *Arch Biochem Biophys*, 353:116–30.
- [30] Alberty, R. A. (2000). Calculating apparent equilibrium constants of enzyme-catalyzed reactions at pH 7. *Biochem Educ*, 28:12–17.
- [31] Briggs, G. E. and Haldane, J. B. S. (1925). A note on the kinetics of enzyme action. *Biochem J*, 19:338–339.
- [32] Michaelis, L. and Menten, M. (1913). Die Kinetik der Invertinwirkung. *Biochem Z*, 49:333–369.
- [33] Cha, S. (1968). A simple method for derivation of rate equations for enzyme-catalyzed reactions under the rapid equilibrium assumption or combined assumptions of equilibrium and steady state. *J Biol Chem*, 243:820–5.
- [34] Hofmeyr, J.-H. and Cornish-Bowden, A. (1997). The reversible Hill equation: how to incorporate cooperative enzymes into metabolic models. *CABIOS*, 13:377–385.
- [35] Topham, C. M. and Brocklehurst, K. (1992). In defence of the general validity of the Cha method of deriving rate equations. The importance of explicit recognition of the thermodynamic box in enzyme kinetics. *Biochem J*, 282 (Pt 1):261–5.
- [36] Cortés, A., Cascante, M., Cárdenas, M. L., and Cornish-Bowden, A. (2001). Relationships between inhibition constants, inhibitor concentrations for 50% inhibition and types of inhibition: new ways of analysing data. *Biochem. J.*, 357:263–268.
- [37] Cornish-Bowden, A. (2004). *Fundamentals of Enzyme Kinetics*. Portland Press, London, 3rd edition.
- [38] Kemp, R. G. and Foe, L. G. (1983). Allosteric regulatory properties of muscle phosphofructokinase. *Mol. Cell. Biochem.*, 57:147–154.
- [39] Tornheim, K. and Lowenstein, J. M. (1976). Control of phosphofructokinase from rat skeletal muscle. *J. Biol. Chem.*, 251:7322–7328.

- [40] Gelpí, J. L., Dordal, A., Montserrat, J., Mazo, A., and Cortes, A. (1992). Kinetic studies of the regulation of mitochondrial malate dehydrogenase by citrate. *Biochem J*, 283 (Pt 1):289–97.
- [41] Onsager, L. (1931). Reciprocal relations in irreversible processes II. *Phys. Rev.*, 38:2265–2279.
- [42] Botts, J. and Morales, M. (1953). Analytical description of the effects of modifiers and of enzyme multivalency upon the steady state catalysed reaction rate. *Trans. Faraday Soc.*, 49:696–707.
- [43] Westerhoff, H. V. and Welch, G. R. (1992). Enzyme organization and the direction of metabolic flow: physicochemical considerations. *Curr Top Cell Regul*, 33:361–90.
- [44] Heimberg, H., De Vos, A., Vandercammen, A., Schaftingen, E. V., Pipeleers, D., and Schuit, F. (1993). Heterogeneity in glucose sensitivity among pancreatic beta-cells is correlated to differences in glucose phosphorylation rather than glucose transport. *EMBO J*, 12:2873–9.
- [45] Schnell, S. and Turner, T. E. (2004). Reaction kinetics in intracellular environments with macromolecular crowding: simulations and rate laws. *Prog Biophys Mol Biol*, 85:235–60.
- [46] Stoleriu, I., Davidson, F. A., and Liu, J. L. (2004). Quasi-steady state assumptions for non-isolated enzyme-catalysed reactions. *J Math Biol*, 48:82–104.
- [47] Stoleriu, I., Davidson, F. A., and Liu, J. L. (2005). Effects of periodic input on the quasi-steady state assumptions for enzyme-catalysed reactions. *J Math Biol*, 50:115–32.
- [48] Fell, D. (1996). *Understanding the Control of Metabolism*. Portland Press, London.
- [49] Heinrich, R. and Schuster, S. (1996). *The regulation of cellular systems*. Chapman and Hall, New York.
- [50] Reder, C. (1988). Metabolic control theory: a structural approach. *J Theor Biol*, 135:175–201.
- [51] Ingalls, B. P. and Sauro, H. M. (2003). Sensitivity analysis of stoichiometric networks: an extension of metabolic control analysis to non-steady state trajectories. *J Theor Biol*, 222:23–36.
- [52] Peletier, M. A., Westerhoff, H. V., and Kholodenko, B. N. (2003). Control of spatially heterogeneous and time-varying cellular reaction networks: a new summation law. *J Theor Biol*, 225:477–87.
- [53] Dhooge, A., Govaerts, W., and Kuznetsov, Y. A. (2003). MATCONT: A MATLAB package for numerical bifurcation analysis of ODEs. *ACM Transactions on Mathematical Software*, 29:141–164.
- [54] Hilborn, R. C. (2000). *Chaos and nonlinear dynamics*. Oxford University Press, Oxford, 2nd edition.

- [55] Schuit, F., De Vos, A., Farfari, S., Moens, K., Pipeleers, D., Brun, T., and Prentki, M. (1997). Metabolic fate of glucose in purified islet cells. Glucose-regulated anaplerosis in beta cells. *J Biol Chem*, 272:18572–9.
- [56] Zelent, D., Najafi, H., Odili, S., Buettger, C., Weik-Collins, H., Li, C., Doliba, N., Grimsby, J., and Matschinsky, F. M. (2005). Glucokinase and glucose homeostasis: proven concepts and new ideas. *Biochem Soc Trans*, 33:306–10.
- [57] Trus, M., Warner, H., and Matschinsky, F. (1980). Effects of glucose on insulin release and on intermediary metabolism of isolated perfused pancreatic islets from fed and fasted rats. *Diabetes*, 29:1–14.
- [58] Erecinska, M., Bryla, J., Michalik, M., Meglasson, M. D., and Nelson, D. (1992). Energy metabolism in islets of Langerhans. *Biochim Biophys Acta*, 1101:273–95.
- [59] Goldbeter, A. and Caplan, S. R. (1976). Oscillatory enzymes. *Annu. Rev. Biophys. Bioeng.*, 5:449–476.
- [60] Tornheim, K. (1979). Oscillations of the glycolytic pathway and the purine nucleotide cycle. *J. theor. Biol.*, 79:491–541.
- [61] Hess, B. (1997). Periodic patterns in biochemical reactions. *Q. Rev. Biophys.*, 30:121–176.
- [62] Pralong, W. F., Bartley, C., and Wollheim, C. B. (1990). Single islet beta-cell stimulation by nutrients: relationship between pyridine nucleotides, cytosolic Ca²⁺ and secretion. *EMBO J*, 9:53–60.
- [63] Longo, E. A., Tornheim, K., Deeney, J. T., Varnum, B. A., Tillotson, D., Prentki, M., and Corkey, B. E. (1991). Oscillations in cytosolic free Ca²⁺, oxygen consumption, and insulin secretion in glucose-stimulated rat pancreatic islets. *J Biol Chem*, 266:9314–9.
- [64] Pralong, W. F., Spat, A., and Wollheim, C. B. (1994). Dynamic pacing of cell metabolism by intracellular Ca²⁺ transients. *J Biol Chem*, 269:27310–4.
- [65] Nilsson, T., Schultz, V., Berggren, P.-O., Corkey, B. E., and Tornheim, K. (1996). Temporal patterns of changes in ATP/ADP ratio, glucose 6-phosphate and cytoplasmic free Ca²⁺ in glucose-stimulated pancreatic β -cells. *Biochem. J.*, 314:91–94.
- [66] Jung, S.-K., Kauri, L. M., Qian, W.-J., and Kennedy, R. T. (2000). Correlated oscillations in glucose consumption, oxygen consumption and intracellular free Ca²⁺ in single islets of langerhans. *J. Biol. Chem.*, 275:6642–6650.
- [67] Deeney, J. T., Köhler, M., Kubik, K., Brown, G., Schultz, V., Tornheim, K., Corkey, B. E., and Berggren, P.-O. (2001). Glucose-induced metabolic oscillations parallel those of Ca(2+) and insulin release in clonal insulin-secreting cells. A multiwell approach to oscillatory cell behavior. *J. Biol. Chem.*, 276:36946–36950.

- [68] Ainscow, E. K. and Rutter, G. A. (2002). Glucose-stimulated oscillations in free cytosolic ATP concentration imaged in single islet beta-cells: evidence for a Ca^{2+} -dependent mechanism. *Diabetes*, 51 Suppl 1:S162–70.
- [69] Bergsten, P., Westerlund, J., Liss, P., and Carlsson, P. O. (2002). Primary in vivo oscillations of metabolism in the pancreas. *Diabetes*, 51:699–703.
- [70] Juntti-Berggren, L., Webb, D. L., Arkhammar, P. O., Schultz, V., Schweda, E. K., Tornheim, K., and Berggren, P. O. (2003). Dihydroxyacetone-induced oscillations in cytoplasmic free Ca^{2+} and the ATP/ADP ratio in pancreatic beta-cells at substimulatory glucose. *J Biol Chem*, 278:40710–6.
- [71] Ristow, M., Carlqvist, H., Heibnick, J., Vorgerd, M., Krone, W., Pfeiffer, A., Müller-Wieland, D., and Östenson, C.-G. (1999). Deficiency of phosphofructo-1-kinase/muscle subtype in humans is associated with impairment of insulin secretory oscillations. *Diabetes*, 48:1557–1561.
- [72] Shimizu, T., Parker, J. C., Najafi, H., and Matschinsky, F. M. (1988). Control of glucose metabolism in pancreatic β -cells by glucokinase, hexokinase, and phosphofructokinase. Model study with cell lines derived from β -cells. *Diabetes*, 37:1524–1530.
- [73] Trus, M. D., Zawulich, W. S., Burch, P. T., Berner, D. K., Weill, V. A., and Matschinsky, F. M. (1981). Regulation of glucose metabolism in pancreatic islets. *Diabetes*, 30:911–922.
- [74] Yaney, G. C., Schultz, V., Cunningham, B. A., Dunaway, G. A., Corkey, B. E., and Tornheim, K. (1995). Phosphofructokinase isozymes in pancreatic islets and clonal β -cells (INS-1). *Diabetes*, 44:1285–1289.
- [75] Eto, K., Tsubamoto, Y., Terauchi, Y., Sugiyama, T., Kishimoto, T., Takahashi, N., Yamauchi, N., Kubota, N., Murayama, S., Aizawa, T., Akanuma, Y., Aizawa, S., Kasai, H., Yazaki, Y., and Kadowaki, T. (1999). Role of NADH shuttle system in glucose-induced activation of mitochondrial metabolism and insulin secretion. *Science*, 283:981–5.
- [76] Albe, K. R., Butler, M. H., and Wright, B. E. (1990). Cellular concentrations of enzymes and their substrates. *J. theor. Biol.*, 143:163–195.
- [77] Zhou, Y. P. and Grill, V. E. (1994). Long-term exposure of rat pancreatic islets to fatty acids inhibits glucose-induced insulin secretion and biosynthesis through a glucose fatty acid cycle. *J Clin Invest*, 93:870–6.
- [78] Lu, D., Mulder, H., Zhao, P., Burgess, S. C., Jensen, M. V., Kamzolova, S., Newgard, C. B., and Sherry, A. D. (2002). ^{13}C NMR isotopomer analysis reveals a connection between pyruvate cycling and glucose-stimulated insulin secretion (GSIS). *Proc Natl Acad Sci U S A*, 99:2708–13.
- [79] Schuster, S., Kahn, D., and Westerhoff, H. V. (1993). Modular analysis of the control of complex metabolic pathways. *Biophys Chem*, 48:1–17.
- [80] Eto, K., Tsubamoto, Y., and Kadowaki, T. (2000). NADH Shuttle and Insulin Secretion. *Science*, 287:931.

- [81] Lee, Y., Hirose, H., Ohneda, M., Johnson, J. H., McGarry, J. D., and Unger, R. H. (1994). Beta-cell lipotoxicity in the pathogenesis of non-insulin-dependent diabetes mellitus of obese rats: impairment in adipocyte-beta-cell relationships. *Proc Natl Acad Sci U S A*, 91:10878–82.
- [82] Zhou, Y. P., Berggren, P. O., and Grill, V. (1996). A fatty acid-induced decrease in pyruvate dehydrogenase activity is an important determinant of beta-cell dysfunction in the obese diabetic db/db mouse. *Diabetes*, 45:580–6.
- [83] MacDonald, M. J., Fahien, L. A., Buss, J. D., Hasan, N. M., Fallon, M. J., and Kendrick, M. A. (2003). Citrate oscillates in liver and pancreatic beta cell mitochondria and in INS-1 insulinoma cells. *J Biol Chem*, 278:51894–900.
- [84] Friesen, W. O. and Block, G. D. (1984). What is a biological oscillator? *Am J Physiol*, 246:R847–53.
- [85] Chay, T. R. and Keizer, J. (1983). Minimal model for membrane oscillations in the pancreatic beta-cell. *Biophys J*, 42:181–90.
- [86] Sherman, A. (1996). Contributions of modeling to understanding stimulus- secretion coupling in pancreatic β -cells. *Am. J. Physiol.*, 271:E362–E372.
- [87] Bertram, R., Satin, L., Zhang, M., Smolen, P., and Sherman, A. (2004). Calcium and glycolysis mediate multiple bursting modes in pancreatic islets. *Biophys J*, 87:3074–87.
- [88] Smolen, P. (1995). A model for glycolytic oscillations based on skeletal muscle phosphofructokinase kinetics. *J. theor. Biol.*, 174:137–148.
- [89] Keizer, J. and Magnus, G. (1989). ATP-sensitive potassium channel and bursting in the pancreatic beta cell. A theoretical study. *Biophys J*, 56:229–42.
- [90] Simon, H. A. (1962). The Architecture of Complexity. *Proceedings of the American Philosophical Society*, 106:467–482.
- [91] Hartwell, L. H., Hopfield, J. J., Leibler, S., and Murray, A. W. (1999). From molecular to modular cell biology. *Nature*, 402:C47–52.
- [92] Magnus, G. and Keizer, J. (1997). Minimal model of β -cell mitochondrial Ca^{2+} handling. *Am. J. Physiol.*, 273:C717–C733.
- [93] Schulze, D., Rapedius, M., Krauter, T., and Baukrowitz, T. (2003). LC-CoA esters and PIPs modulate ATP inhibition of KATP channels by the same mechanism. *J Physiol*, 552:357–67.
- [94] Mayr, G. W. and Heilmeyer Jr, L. M. G. (1983). Phosphofructokinase is a calmodulin binding protein. *FEBS Lett.*, 159:51–57.
- [95] Straub, S. G. and Sharp, G. W. (2004). Hypothesis: one rate-limiting step controls the magnitude of both phases of glucose-stimulated insulin secretion. *Am J Physiol Cell Physiol*, 287:C565–71.

- [96] Grodsky, G. M. (1972). A threshold distribution hypothesis for packet storage of insulin and its mathematical modeling. *J. Clin. Invest.*, 51:2047–2059.
- [97] Grodsky, G. M. (1972). A threshold distribution hypothesis for packet storage of insulin II. Effect of calcium. *Diabetes*, 21 (Suppl. 2):584–593.
- [98] Massa, L., Baltrusch, S., Okar, D. A., Lange, A. J., Lenzen, S., and Tiedge, M. (2004). Interaction of 6-phosphofructo-2-kinase/fructose-2,6-bisphosphatase (PFK-2/FBPase-2) with glucokinase activates glucose phosphorylation and glucose metabolism in insulin-producing cells. *Diabetes*, 53:1020–9.
- [99] Gerbitz, K. D., Gempel, K., and Brdiczka, D. (1996). Mitochondria and diabetes. Genetic, biochemical, and clinical implications of the cellular energy circuit. *Diabetes*, 45:113–26.
- [100] Sherman, A., Rinzel, J., and Keizer, J. (1988). Emergence of organized bursting in clusters of pancreatic beta-cells by channel sharing. *Biophys. J.*, 54:411–425.
- [101] Hellman, B., Dansk, H., and Grapengiesser, E. (2004). Pancreatic beta-cells communicate via intermittent release of ATP. *Am J Physiol Endocrinol Metab*, 286:E759–65.
- [102] Winfree, A. T. (2002). Oscillating systems. On emerging coherence. *Science*, 298:2336–7.